Menoufia University

Faculty of Science
Mathematics Department

Applications of the Variational Monte Carlo Method to the Two Atoms Molecules

A THESIS

Submitted to Mathematics Department, Faculty of Science, Menoufia University

In Partial Fulfillment of the requirements for the Master Degree of Science

(M. Sc. in Applied Mathematics)

By

Asmaa Abd El-Moghney Abd El-Aziz Amer

Demonstrator of Mathematics, Department of Mathematics,
Faculty of Science, Menoufia University

Supervisors

Professor Dr. Salah El-Din Badawi Doma

Professor of Applied Mathematics,
Department of Mathematics, Faculty of Science,
Alexandria University

Dr. Mohamed Mohamed Abu-Shady

Assistant Professor of Applied Mathematics,
Department of Mathematics, Faculty of Science
Menoufia University

Dr. Fatma El-Zahraa Nageeb El–Gammal

Lecturer of Applied Mathematics,
Department of Mathematics, Faculty of Science
Menoufia University

Examiners Committee

Professor Dr. Mohamed Omar Shaker
Professor of Applied Mathematics,
Department of Mathematics, Faculty of Science,
Tanta University
[ ]

Professor Dr. Nabil Tawfik El-Daba
Professor of Applied Mathematics,
Department of Mathematics, Faculty of Education,
Ain Shams University
[ ]

Professor Dr. Salah El-Din Badawi Doma
Professor of Applied Mathematics,
Department of Mathematics, Faculty of Science,
Alexandria University
[ ]

Dr. Mohamed Mohamed Abu-Shady
Assistant Professor of Applied Mathematics,
Department of Mathematics, Faculty of Science,
Menoufia University
[ ]

EGYPT
2015

ACKNOWLEDGMENT

First of all I would like to thank **ALLAH** for helping me to complete this work.

This work would not have been possible if it weren't for the help, guidance, and friendship of many people. My advisor, **Professor Dr. Salah El-Din Badawi Doma,** Professor of Applied Mathematics, Faculty of Science, Alexandria University, who has been an invaluable source of guidance, patience and support during elaborating this work.

I would like to express my deep thanks to **Dr. Mohamed Mohamed Abu-shady,** Assistant Professor of Applied Mathematics, Faculty of Science, Menoufia University and **Dr. Fatma Elzahraa Nageeb El-Gammal**, Lecturer of Applied Mathematics, Faculty of Science, Menoufia University, for their supervision, valuable discussion and encouragement.

My sincere thanks are dedicated to everyone who give me help and support to finish this thesis, especially, **Professor Dr. Mohamed Amin Abdelwahed** (The head of Mathematics Department) and **Dr. Weal Saleh Amer**, Lecturer of Applied Mathematics, Faculty of Science, Menoufia University.

I am highly appreciative of the support and encouragement provided by my colleagues and my friends in the Department of Mathematics and in Faculty of Science.

Outside of the college, my family has been a constant source of support. Thanks go out especially to my **father**, my brother's **Abd El-Aziz**, **Mohamed** and **Ahmed**, and my sister **Esraa**.

Asmaa Abd El-Moghney Amer

ABSTRACT

In this thesis, the ground state energies of the hydrogen molecular ion H_2^+ and the hydrogen molecule H_2 are numerically evaluated using the variational Monte Carlo method. The Case of the hydrogen molecular ion H_2^+ and the hydrogen molecule H_2 compressed by spherical hard wall is studied. Our study were extended also to include the HeH^{++} molecular ion. Finally, we have calculated the total energies, the dissociation energies, and the binding energies for the hydrogen molecular ion H_2^+ and the hydrogen molecule H_2 in the presence of external magnetic field in the framework of a variational Monte Carlo (VMC) method. All cases of our results exhibit good accuracy comparing with previous values using different methods and different forms of the trial wave functions. In this way we conclude that the applications of VMC method can be extended successfully to cover other characteristics of molecules.

SUMMARY

The aim of this thesis is to investigate the ground state characteristics of the hydrogen molecule, the confined hydrogen molecule, the hydrogen molecular ion and the confined hydrogen molecular ion in the absence and in the presence of aligned magnetic field. For these purposes we have applied the variational Monte Carlo method, which has been previously applied successfully for the ground and excited states of the helium and lithium atoms. The Metropolis algorithm has been adopted in our calculations with the well known Born-Oppenheimer approximation. Accurate and compact trial wave functions have been used for this purpose.

The present thesis consists of five chapters and is organized as follows:

Chapter One

In this chapter we introduced the essential outlines of the topics investigated in the present thesis, especially the history of the Monte Carlo methods which are dealing with the atomic and molecular systems. Also, we presented a historical review about the Schrödinger equation and its applications in these two branches. This chapter is ended by the literature review.

Chapter Two

In chapter two we have introduced the formulation of the variational Monte Carlo (VMC) method which is based on a combination of the variational principle and the Monte Carlo evaluation of integrals, using importance sampling based on the Metropolis algorithm. Furthermore, we have explained the Metropolis algorithm, its logical steps and its acceptance and rejection ideas. Also, we have introduced the important

role of the trial wave function in the variational method generally and in the variational Monte Carlo method especially.

Chapter Three

In this chapter we have used the variational Monte Carlo method to calculate the ground state energies of the hydrogen molecular ion H_2^+ and the hydrogen molecule H_2 at different interproton separation distance. The calculations were carried out in framework of the principles of the Born-Oppenheimer approximation, the approximation which considers the case of an infinitely heavy nucleus**.** We also presented in this chapter a survey of the trial wave functions which are used in our calculations of the energy eigenvalues of the different molecular systems tackled in this thesis. Our calculations gave good results in comparison with the most recent data and the comparison showed that the accuracy and efficiency of the VMC method in calculating different molecular properties of hydrogen molecule H_2 and its molecular ion H_2^+ are very clear.

Chapter Four

This chapter is devoted to investigate the applications of the variational Monte Carlo method to the calculations of the ground state energy of the hydrogen molecule H_2 and the hydrogen molecular ion H_2^+ confined by a hard prolate spheroidal cavity. In these investigations the case where the nuclear positions are clamped at the foci (on-focus case) is considered. Also, the case of off-focus nuclei in which the two nuclei are not clamped to the foci is studied. Accurate trial wave functions depending on many variational parameters are used for these purposes. The results were extended also to include the HeH^{++} molecular ion. The obtained results are in good agreement with the most recent results. In all cases our results

exhibit a good accuracy comparing with previous values using different methods and different forms of the trial wave functions.

Chapter Five

In chapter five we have applied the variational Monte Carlo method to calculate the $1s\sigma_g$ state energies, the dissociation energies, and the binding energies of the hydrogen molecular ion H_2^+ and the hydrogen molecule H_2 in the presence of an aligned magnetic field regime between 0 a.u. and 10 a.u. Our calculations are based on using compact and accurate trial wave functions. The obtained results are compared with the most recent accurate values and have shown excellent agreement with these results.

List of Figures

Figure Name ***Page No.***

List of Tables

Table Name ***Page No.***

List of Contents

Chapter 1

Introduction

The history of Monte Carlo methods goes back a long time. The generic idea of random, or "stochastic", sampling is straightforward and appealing in its elegance and has been used for centuries. Possibly the first systematic application of statistical sampling techniques in science and engineering was by Enrico Fermi in the early 1930's to predict the results of experiments related to the properties of the neutron [1] which had recently been discovered by James Chadwick in 1932.

In 1947, Stanislaw Ulam suggested to John Von Neumann that the newly developed ENIAC computer would give them the means to carry out calculations based on statistical sampling with hitherto unattained efficiency and comparative ease [2]. Their coworker Nicholas Metropolis dubbed the numerical technique "the Monte Carlo method" parly inspired by Ulam's anecdotes of his gambling uncle who just had to go to Monte Carlo. Since the deployment of the ENIAC which could do about 5000 additions or 400 multiplications per second and occupied the size of a large room, computing power has grown dramatically.

In the early 1970's, a computer design was introduced that had at its heart an electronic component first introduced in 1958, a so-called "integrated circuit". All of a sudden, a computer's Central Processing Unit shrank from the size of a domestic refrigerator to that of a fingernail. The number of transistors in a single integrated circuit kept growing at an almost constant exponential rate since then, and with it grew the computing power of the computer. In addition to that, miniaturization and

the introduction of new materials allowed for equally dramatic increases in computer's clock speeds.

For the recent CPU-computer devices, 2 billion double precision floating point multiplications can be carried out per second which means that the kind of hardware used these days as a word processor can do in one second what used to take the ENIAC over two months. It is no surprise, then, that by now the use of Monte Carlo (MC) methods has become ubiquitous in science, technology and business.

Simulation techniques are used in: oil well exploration; stellar evolution; electronic chip design; reactor design; quantum chromo dynamics; material sciences; physical chemistry; nanostructure, protin, and polymer research; operations research, e. g., when designing the relationships and control mechanisms between raw materials input, manufacturing, and delivery; ground and air traffic control systems design; communication and computer system design and testing, e.g., network theory; bimolecular research, e. g., cancer drug design; all areas of finance and insurance; weather forecasting (where it is referred to as "ensemble forecasting"); and local authorities planning and commissioning site.

Recently, Quantum Monte Carlo (QMC) have become a powerful tool in Quantum Mechanics calculations because it provides a practical method for solving the many-body Schrödinger equation. It is commonly used in physics to simulate complex systems that are of random nature in statistical physics. The term QMC refers to group of methods in which physical or mathematical problems are simulated by using random numbers.

QMC methods are ones of the most accurate for computing the properties of liquids and solids for interacting Hamiltonians [3, 4]. These

methods do not require approximation, and can be used to solve Hamiltonians exactly.

MC methods can be used to simulate quantum mechanical systems, but are also well suited for calculating integrals, especially high-dimensional integrals.

There are many versions of the QMC methods that are used to solve the Schrödinger equation for the ground state energy of a quantum system including the diffusion Monte Carlo (DMC) method [5], which is used to solve the time-dependent Schrödinger equation. Another method is the Green's function Monte Carlo which has been extended [6] to multiple states with the same quantum numbers. The simplest of QMC methods is the variational Monte Carlo (VMC) method which has become a valuable tool of the quantum chemist calculations.

Recently, VMC method was used widely to calculate both ground and excited states for atoms and molecules. The obtained results are of good agreement with the exact data. The major advantage of this method is the possibility of freely choose the analytical form of the trial wave function which may contain highly sophisticated term in such a way that electron correlation is explicitly taken into account.

In general, QMC methods use a stochastic integration method to evaluate expectation values for a chosen trial wave function. In a system of 1000 electrons the required integrals are 3000 dimensional and for such problems MC integration is much more efficient than conventional quadrature methods such as Simpson's rule. The main drawback of QMC is that the accuracy of the result depends entirely on the accuracy of the trial wave function.

In general, MC methods are especially useful in studying systems with a large number of coupled degrees of freedom, such as liquids, strongly coupled solids, and cellular structure. Moreover, VMC method has been

widely applied not only to strongly interacting lattice systems, but also to realistic continuous models, such as electron gas [5], quantum dots [6], nanoclusters [7], solid hydrogen [8] and liquid helium.

The applications of VMC method are also extended to include some medical applications because it is the most accurate way to simulate radiation transport on a computer. Also, it will help doctor to choose a treatment that maximized the radiation dose to the tumor and minimizes the dose to normal tissues [9].

In telecommunications, when planning a wireless network, design must be proved to work for a wide variety of scenarios that depend mainly on the number of users, their locations and the services they want to use. MC methods are typically used to generate these users and their states. The network performance is then evaluated and, if results are not satisfactory, the network design goes through an optimization process.

MC methods are very important in computational physics, physical chemistry, and related applied fields, and have diverse applications from complicated quantum chromodynamics calculations to designing heat shields and aerodynamic forms as well as in modeling radiation transport for radiation dosimetry calculations. In statistical physics MC molecular modeling is an alternative to computational molecular dynamics, and MC methods are used to compute statistical field theories of simple particle and polymer systems.

MC methods solve the many-body problem for quantum systems. In experimental particle physics, MC methods are used for designing detectors, understanding their behavior and comparing experimental data to theory.

In astrophysics, they are used in such diverse manners as to model both the evolution of galaxies and the transmission of microwave

radiation through a rough planetary surface. MC methods are also used in the ensemble models that form the basis of modern weather forecasting.

MC methods in finance are often used to evaluate investments in projects at a business unit or corporate level, or to evaluate financial derivatives. They can be used to model project schedules, where simulations aggregate estimates for worst-case, best-case, and most likely durations for each task to determine outcomes for the overall project.

In general, VMC method are used in mathematics to solve various problems by generating suitable random numbers (see also Random number generation) and observing that fraction of the numbers that obeys some property or properties. The method is useful for obtaining numerical solutions to problems too complicated to solve analytically. The most common application of the MC method is MC integration.

The Schrödinger equation is the name of the basic non-relativistic wave equation used in one version of quantum mechanics to describe the behavior of a particle in a field of force.

Schrödinger was the first person who set his mind on finding a wave equation for the electron. Closely following the electromagnetic prototype of a wave equation, and attempting to describe the electron relativistically, he first arrived at what we today know as the Klein-Gordon-equation. To his annoyance, however, this equation, when applied to the hydrogen atom, did not result in energy levels consistent with Arnold Sommerfeld’s fine structure formula, a refinement of the energy levels according to Bohr. Schrödinger therefore retreated to the non-relativistic case, and obtained as the non-relativistic limit to his original equation the famous equation that now bears his name. He published his results in a series of papers in 1926 [10, 11].

Therein, he emphasizes the analogy between electrodynamics as a wave theory of light, which in the limit of small electromagnetic

wavelength approaches ray optics, and his wave theory of matter, which approaches classical mechanics in the limit of small de Broglie wavelengths. His theory was consequently called wave mechanics. In a wave mechanical treatment of the hydrogen atom and other bound particle systems, the quantization of energy levels followed naturally from the boundary conditions. A year earlier, Werner Heisenberg had developed his matrix mechanics, which yielded the values of all measurable physical quantities as eigenvalues of a matrix.

Schrödinger succeeded in showing the mathematical equivalence of matrix and wave mechanics [12]. They are just two different descriptions of quantum mechanics. A relativistic equation for the electron was found by Paul Dirac [13]. It included the electron spin of 1/2, a purely quantum mechanical feature without classical analog. Schrödinger's original equation was taken up by Klein and Gordon, and eventually turned out to be a relativistic equation for bosons, i.e. particles with integer spin. In spite of its limitation to non-relativistic particles, and initial rejection from Heisenberg and colleagues, the Schrödinger equation became eventually very popular. Today, it provides the material for a large fraction of most introductory quantum mechanics courses.

In the case of a few idealized scenarios, the Schrödinger equation may be solved analytically in order to describe the phenomenon of a quantum particle. For other systems the behavior of the quantum particle can become so complex that numerical techniques must be used in order to solve the Schrödinger equation and obtain its eigenfunctions and eigenvalues. The MC method provides a convenient way to solve the Schrödinger equation because of its success in obtaining a probability distribution.

The ground-state energy of a quantum particle may be obtained analytically by solving the Schrödinger equation if the problem is simple

enough for this to be possible. Alternatively, using a variational wave function for the quantum particle, the Schrödinger equation can be solved numerically within a MC method. The MC method makes use of an initial probability distribution to estimate the ground-state energy of the quantum particle. The exact minimum energy of the quantum particle is found by varying the trial wave function. The minimum ground-state energy as a function of the variational parameter identifies the ground state as well as the system's eigenstate. The minimum of the energy must be accompanied by a minimum in the standard deviation.

Literature Review

In this section, we will handle in details the previous work presented in frame work of the MC methods.

Manisa [14] investigated systematic nuclear matter. Total, kinetic and potential energies per particle were obtained for nuclear matter by VMC method. They had observed that the results were in good agreement with those obtained by various authors who used different potentials and techniques.

Ma *et al*. [15] presented all electron variational and diffusion (VMC and DMC) calculations for the noble gas atoms He, Ne, Ar, Kr, and Xe. The calculations were performed using Slater-Jastraw wave functions with Hartree-Fock single-particle orbitals. The quality of both the optimized factors and the nodal surfaces of the wave functions declines with increasing atomic number Z. They discussed the scaling of the computational cost of the DMC calculations with Z.

Chiesa *et al*. [16] reported that computation of ionic forces using QMC had long been a challenge. They introduced a simple procedure, based on known properties of physical electronic densities, to make the variance of the Hellmann-Feynman estimate finite. They obtained very accurate geometries for the molecules H_2, LiH, CH_4, NH_3, H_2o, and HF, with a Slater-Jastraw trial wave function. Harmonic frequencies for diatomic also are in good agreement with experiment.

Drummond *et al*. [17] reported all electron and pseudopotential calculations of the ground-state energies of the neutral Ne atom and the Ne^+ ion using the variational and diffusion quantum Monte Carlo (VQMC and DQMC) methods. They investigated different levels of Slater-Jastraw trial wave function: (i) using Hartree- Fock orbitals, (ii) using orbitals optimized within a Monte Carlo procedure in the presence of a Jastraw

factor, and (iii) including backflow correlations in the wave function. Small reductions in the total energy were obtained by optimizing the orbitals, while more significant reductions were obtained incorporating backflow correlations.

Davis [18] used the VMC method to study the electronic structure of atomic hydrogen, helium, lithium, and beryllium. The trial functions were taken as products of hydrogenic orbitals for which Z is treated as a variable parameter. The variationally optimized values of these parameters are interpreted as effective nuclear charges. The results were used to explicate several features of many electron atoms, including electron shielding in the ground state of helium, singlet–triplet splitting in the first excited state of helium, the difference in 2s and 2p penetration in lithium, and the trends in ionization energies for Be, Be^{+}, and Be^{2+}.

Brown *et al*. [19] calculated the ground state energies of the first row atoms (Li to Ne) by using VQMC and DQMC calculations. They used trial wave functions of types: single determinant Slater-Jastraw wave functions; multi-determinant Slater-Jastraw wave functions with backflow transformations.

In Ref [20], the VMC method was used to study the linear and periodic chain of hydrogen atoms. The calculations were based on using a highly correlated Jastrow antisymmetrized geminal power variational wave function. It was proven that the accuracy of the calculations were comparable to that of benchmark density matrix renormalization-group calculations. Furthermore, the crossover between the weakly and strongly correlated regimes of this atomic chain was characterized using the so-called “modern theory of polarization” and by studying the spin-spin and dimer-dimer correlations functions. The obtained results show that the VMC method provides an accurate and flexible alternative to highly correlated methods of quantum chemistry which, at variance with these

methods, can be also applied to a strongly correlated solid in low dimensions close to a crossover or a phase transition.

Barborini *et al*. [21] presented full structural optimizations of the ground state and of the low lying triplet state of the ethylene molecule by means of QMC methods. All of the calculations were done using an accurate and compact wave function based on Pauling's resonating valence band representation: the Jastraw Antisymmetrized Geminal Power (JAGP). Bond lengths and bond angles were calculated with a statistical error of about 0.1% and are in good agreement with the available experimental data.

In Ref [22], VMC method was used to describe spin-orbit splitting in heavy atoms. Calculations were tested first for the light C atom, and then extended to a set of heavier open p-shell atoms (Ti to Po). In frame of the presented results VMC approach introduced an efficient and very accurate way when spin orbit effects are included in the Hamiltonian describing the electronic structure.

In 2012, Mizusaki *et al.* [23] proposed a new VMC method with an energy variance extrapolation to study the large-scale shell-model calculations. Using this method, they could stochastically calculate approximated energies and electro-magnetic transition strengths. The exact shell-model energies were estimated by combining VMC method with energy variance extrapolation.

Elkahwagy *et al.* [24-26] have studied the VMC and the DMC methods. To allow the QMC calculations of the heavy atom, pseudopotential valence-only calculations have been performed, since the presence of the inert core electrons introduces a large fluctuation in the energies and this reduces the computational efficiency. The basic form of the wave function is the Slater-Jastrow wave function which is considered the most common and simplest one.

In paper [24] the authors perform QMC calculations for the ground state energies of both the neutral atoms and their corresponding cations for Ce to Eu in order to evaluate their first ionization potential.

In paper [25] the authors have calculated the ground state energies of La atom and its charged cations with the hope "achieving high accuracy" by using VMC and DMC methods. In addition, they study the DMC energies at different time steps and the accurate extrapolated value of the ground state energy of La atom is derived.

In Ref [26] the authors have performed pseudopotential calculations of the ground state energies of actinium and thorium neutral atoms and some of their corresponding cations by using VMC and DMC methods. The fluctuation of the local energy that has been obtained is found to be below 2 a.u. in all cases under study. Additionally, they study the dependence of DMC energy on the size of the time step for actinium.

Recently, many studies have been presented by Doma *et al.* using the VMC method for atoms. In Ref [27], they evaluated the energy of the ground state of the helium atom where the relativistic effect was taken into account. Also, they extended their study in Ref [28] to calculate the lowest order relativistic corrections for the ground state energies of the helium-like atoms, up to Z = 10, and also for some excited state energies of the helium atom. These relativistic corrections include: mass-velocity effect, orbit-orbit interaction, spin magnetic and dipole moments of the two electrons and the Darwin effect. Moreover, correction due to the nucleus motion has been also calculated.

In 2012, the case of compressed helium atom by spherical box was studied. For various values of the spherical box radii, Doma *et al.* [29] have calculated the energies for both helium and its isoelectronic ions, Li^+ and Be^{2+}. They considered the case of small values of r_c, which describe the strong compression, as well as the case of large values of r_c. In both

cases, the results exhibit good accuracy compared with previous values using different methods and different forms of trial wave functions.

For lithium atom, VMC presented an efficient technique for calculating the ground state energy and its ion up to Z=10 [30]. Also, Doma in [31] investigated the effect of an external magnetic field on the ground state energies of the helium atom, and hydrogen negative ion. The obtained results were in good agreement with the most recent previous accurate values and also with the exact values.

Chapter 2

The Variational Monte Carlo Method

2.1 Formulation of the Method

In this section we summarize the strategy used to calculate the expectation value of any operator using variational Monte Carlo (VMC) method. The term VMC is derived from the use of Monte Carlo type in conjunction with the variational principle. VMC is based on a combination of two ideas namely the variational principal and the Monte Carlo evaluation of integrals using importance sampling based on the Metropolis algorithm. During the last ten years it has become clear that VMC can produce very accurate ground and excited states expectation values for atoms and molecules. For a sufficiently high number of variables in the integrand, VMC method are much more efficient than a deterministic integration such as Simpson's rule, and the many-body systems are certainly the case. The VMC methods are used to compute quantum expectation values of an operator with a given trial wave function. In particular, if the operator is the Hamiltonian, its expectation value is the varitional energy

$$E_{VMC} = \frac{\langle \psi_T | \hat{H} | \psi_T \rangle}{\langle \psi_T | \psi_T \rangle} = \frac{\int \psi_T^*(\boldsymbol{R})\, \hat{H}\, \psi_T(\boldsymbol{R})\, d\boldsymbol{R}}{\int \psi_T^*(\boldsymbol{R})\, \psi_T(\boldsymbol{R})\, d\boldsymbol{R}} \tag{2.1}$$

where ψ_T is a trial wave function and $\boldsymbol{R}$ is the $3N$-dimensional vector of the electron coordinates. According to the variational principle, a trial wave function for a given state must produce an energy which is above the exact value of that state; i.e. $E_{VMC} \geq E_{exact}$. To evaluate the integral in Eq. (2.1) we firstly construct a trial wave function, $\psi_T^{\propto}(\boldsymbol{R})$, depending on a set of $\propto$-variational parameters $\propto = (\propto_1, \propto_2, \ldots, \propto_N)$ and then vary

the parameters to obtain minimum energy. The VMC method is a Monte Carlo method for evaluating the multi-dimensional integral in Eq. (2.1). This is achieved by rewriting Eq. (2.1) in the following form,

$$E_{VMC} = \frac{\int |\psi_T(\boldsymbol{R})|^2 \frac{\hat{H}\psi_T(\boldsymbol{R})}{\psi_T(\boldsymbol{R})} d\boldsymbol{R}}{\int |\psi_T(\boldsymbol{R})|^2 d\boldsymbol{R}} \tag{2.2}$$

VMC calculations determine E_{VMC} by writing it as [7]

$$E_{VMC} = \int P(\boldsymbol{R})\, E_L(\boldsymbol{R})\, d\boldsymbol{R} \tag{2.3}$$

where $P(\boldsymbol{R}) = \frac{|\psi_T(\boldsymbol{R})|^2}{\int |\psi_T(\boldsymbol{R})|^2\, d\boldsymbol{R}}$ is positive everywhere and interpreted as a probability distribution and $E_L = \frac{\hat{H}\psi_T(\boldsymbol{R})}{\psi_T(\boldsymbol{R})}$ is the local energy function.

The value of E_L is evaluated using a series of points $\boldsymbol{R}_{ij}$ sampled from the probability density $P(\boldsymbol{R})$. At each of these points the weighted average $\langle E_L \rangle = \frac{\int \psi_T^2(\boldsymbol{R})\, E_L\, d\boldsymbol{R}}{\int \psi_T^2(\boldsymbol{R})\, d\boldsymbol{R}}$, is evaluated. After a sufficient number of evaluations the VMC estimate of E_{VMC} will be

$$E_{VMC} = \langle E_L \rangle = \lim_{N\to\infty} \lim_{M\to\infty} \frac{1}{N} \frac{1}{M} \sum_{j=1}^{N} \sum_{i=1}^{M} E_L\left(\boldsymbol{R}_{ij}\right) \tag{2.4}$$

where M is the ensemble size of random numbers $\{\boldsymbol{R}_1, \boldsymbol{R}_2, \ldots, \boldsymbol{R}_M\}$, which may be generated using a variety of methods [32, 33] and N is the number of ensembles. These ensembles so generated must reflect the distribution function itself. A given ensemble is chosen according to the Metropolis algorithm [34]. This method uses an acceptance and rejection process of random numbers that have a frequency probability distribution like ψ^2. The acceptance and rejection method is performed by obtaining a random number from the probability distribution, $P(\boldsymbol{R})$, then testing its value to determine if it will be acceptable for use in approximating the local energy. After an ensemble of random numbers is generated, the acceptance criterion is such that the probability of moving from an initial random number of the ensemble, $\boldsymbol{R}_i$, to a new random number, $\boldsymbol{R}_k$, is defined according to the ratio

$$\mathrm{A} = \frac{\psi^2(\boldsymbol{R_k})}{\psi^2(\boldsymbol{R_i})} \tag{2.5}$$

If A is larger than one, this trial step is accepted (i.e. we put $\boldsymbol{R}_{i+1} = \boldsymbol{R}_k$) and the new $\boldsymbol{R}_k$ is a member of the next ensemble. While if A is less than one, the step is accepted with probability A.

If the trial step is not accepted, then it is rejected, and we put $\boldsymbol{R}_{i+1} = \boldsymbol{R}_i$. This process is repeated for each member of an ensemble and is done in order to broaden subsequent ensembles for a wider sampling range. Any arbitrary point $\boldsymbol{R}_0$ can be used as the starting point for the random walk.

The accepted ensembles will be used to evaluate the VMC estimate for the average energy according to Eq. (2.4). In our work the broadening of the ensemble is achieved according to

$$\boldsymbol{Y} = \boldsymbol{R}(K) + DELTA * (RAND0\ (SEED) - 0.5) \tag{2.6}$$

where $\boldsymbol{Y}$ is the new value $\boldsymbol{R}_k$ to be tested and $\boldsymbol{R}(K)$ is the value $\boldsymbol{R}_i$ of the previously accepted ensemble for $K = i$.

The function $RAND$ returns a uniform random number between 0 and 1, and is a nonintrinsic function. The range width is determined by $DELTA$, adjusted to suit particular needs, and the value 0.5 ensures the availability of negative numbers. The random number generator only produces numbers between 0 and 1, so there will be an initial maximum random value and an initial minimum random value. These maximum and minimum values in the new accepted ensemble, $\{\boldsymbol{R}(K)\}$, are kept as subsequent ensemble grows in range. Finally, it is important to calculate the standard deviation of the energy [7]

$$\sigma = \sqrt{\frac{\langle E_L^2\rangle - \langle E_L\rangle^2}{L\ (N-1)}} \tag{2.7}$$

2.2 The Metropolis Algorithm

The Metropolis Algorithm has been the most successful and influential of all the members of the computational species that called the Monte Carlo Method. This method we have used to sample points from the chosen probability distribution is the Metropolis algorithm. The Metropolis algorithm was named after Nicholas Metropolis, who was an author along with A. W. Rosenbluth, M. N. Rosenbluth, A. H. Teller and E. Teller of the 1953 paper "*Equation of State Calculations by Fast Computing Machines*" [34] which was the first that proposed algorithm for the specific case of the canonical ensemble. It is well-known also that W. K. Hastings [34] was the first who extended this algorithm to the more general case in 1970.

Whereas the context in which it was invented is now largely irrelevant, this powerful technique continues to be a versatile tool in a great many numerical simulations in several different branches of science [35, 36]. The Metropolis algorithm is the most widely used algorithm for generating a sequence of points that sample a given probability distribution to sample physical quantities such as the total energy efficiently.

In the QMC method each point in the phase space is a vector $\boldsymbol{R} = (\boldsymbol{r}_1, \boldsymbol{r}_2, \dots, \boldsymbol{r}_N)$ in the 3N-dimensional space of the position coordinates of all the N electrons, and the sequence of phase space points provides a statistical representation of the ground state of the system. If we are to build up a statistical picture of the overall system of electrons and nuclei, it is necessary to move the electrons around to cover all possible positions and hence all possible states of the system. As we move the electrons around, we can keep track of physical quantities such as the total energy, polarisation, etc., associated with the instantaneous state of the electron configuration. The sequence of individual samples of these quantities can

be combined to arrive at average values which describe the quantum mechanical state of the system. Many pseudo-random numbers are used to generate the sequence of states, which are collectively called a random walk.

In Metropolis algorithm, a random walk is performed through the configuration space of interest. The walk is designed so that the points on the walk are distributed according to the required probability distribution. At each point on the walk a random trial move from the current position in configuration space is selected. This trial move is then either accepted or rejected according to a simple probabilistic rule. If the move is accepted then the "walker" moves to the new position in configuration space; otherwise the "walker" remains where it is, (By a "walker" we mean a point in the 3N-dimensional configuration space of the problem).

Another trial step is then chosen, either from the new accepted position or from the old position if the first move was rejected, and the process is repeated. In this way it should be possible for the "walker" to explore the whole configuration space of the problem. The Metropolis algorithm provides a prescription for choosing which moves in configuration space to accept or reject. In this algorithm, a random walk is performed through the configuration space of interest. The walk is designed so that the points on the walk are distributed according to the required probability distribution. At each point on the walk a random trial move from the current position in configuration space is selected.

The metropolis algorithm is able to compute the averages over a sequence of sampling point $(\boldsymbol{r}_1, \boldsymbol{r}_2, \dots, \boldsymbol{r}_N)$ generated by moving a single walker, according to the following rules:

1- Start the walker at a random position R_n.

2- Make a trial move to a new position R_{n+1} chosen from some probability density function $P_{trial}(R_n \to \acute{R})$.

3- Accept the trial move to $\acute{R}$ with probability:

$$P_{accept}(R_n \to \acute{R}) = min\left\{1, \frac{P_{trial}(\acute{R} \to R_n)P(\acute{R})}{P_{trial}(R_n \to \acute{R})P(R_n)}\right\}$$

where $P(R_n)$ is the probability density of finding the electrons in the configuration R_n and $P_{trial}(\acute{R} \to R_n)$ is the trial probability from configuration $\acute{R}$ to R_n.

4- Calculate $A = \frac{P_{trial}(\acute{R} \to R_n)P(\acute{R})}{P_{trial}(R_n \to \acute{R})P(R_n)}$.

5- generate a random number r_n between 0 and 1 and compare it with A.

6- If A$\geq r_n$ the trial move is accepted, otherwise reject it. If the trial move is accepted the point $\acute{R}$ become the next point on the walk ($\acute{R} = R_{n+1}$). If the trial move is rejected the point R_n become the next point on the walk ($R_n = R_{n+1}$).

7- collect averages using the configurations.

8- calculate error bars.

Figure-2.1 displays a flow chart illustrating the Metropolis algorithm and the method of acceptance and rejection.

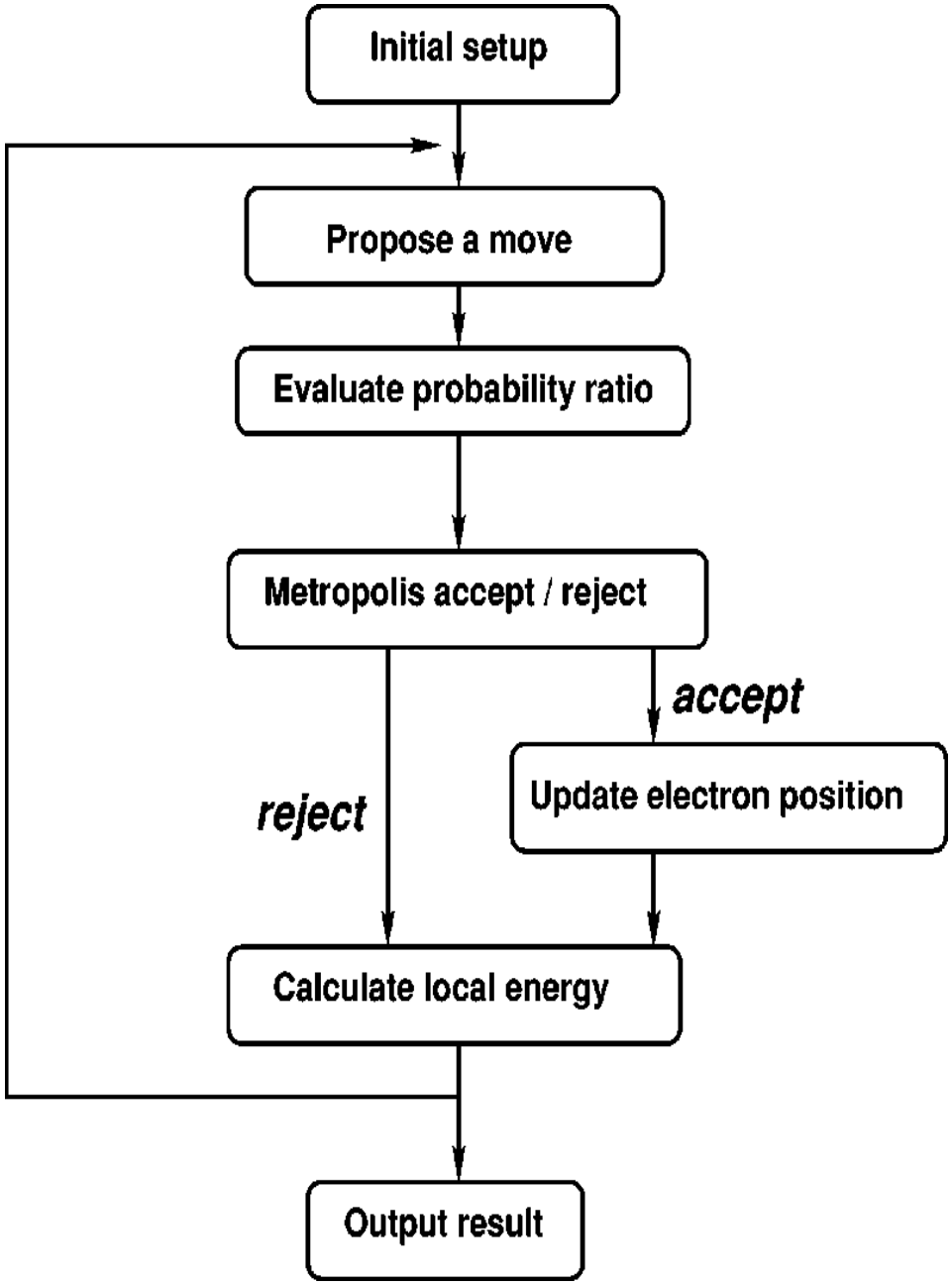

Figure-2.1 Flow chart illustrating the Metropolis algorithm.

2.3 Random Numbers Generations

In all Monte Carlo calculations we need to produce a long sequence of random numbers N_i that are uniformly distributed over the interval [0, 1]. But no numerical algorithms can generate a truly random sequence of numbers; however, there exist algorithms which generate repeating sequences of M (say) integers which, to a fairly good approximation, are randomly distributed in the range 0 to $M-1$. Here M is a (hopefully) large integer. This type of sequence is termed pseudorandom numbers. Pseudorandom number generators (PRNGs) are algorithms that can automatically create long runs of numbers with good random properties but eventually the sequence repeats (or the memory usage grows without bound. The series of values generated by such algorithms is generally determined by a fixed number called a seed. One of the most common PRNG is the linear congruential generator, which uses the recurrence

$$N_{i+1} = (a\,N_i + c)\;mod\;(M) = \text{remainder}\left(\frac{a\,N_i+c}{M}\right)$$

One multiplies the previous random number N_i by the constant a, add another constant c, take the modulus by M and then keep just the fractional part (remainder) as the next random number N_{i+1}

The number M is called the period and it should be as large as possible and N_1 is the starting value, or seed. The function mod means the remainder, that is if we were to evaluate $(13)\;mod\;(9)$, the outcome is the remainder of the division 13/9, namely 4. The problem with such generators is that their outputs are periodic; they will start to repeat themselves with a period that is at most M. If however the parameters a and c are badly chosen, the period may be even shorter.

The value for N_1 (the seed) is frequently supplied by the user, and mod is a built-in function on the computer for remaindering (it may be called amod or dmod). This is essentially a bit-shift operation that ends up with

the least significant part of the input number and thus counts on the randomness of round-off errors to generate a random sequence.

As an example, if $c = 1$, $a = 4$, $M = 9$, and one supplies $N_1 = 3$, then he obtains the sequence

$$N_1 = 3,$$

$$N_2 = (4 \times 3 + 1)\ mod\ 9 = 13\ mod\ 9 = rem\frac{13}{9} = 4,$$

$$N_3 = (4 \times 4 + 1)\ mod\ 9 = 17\ mod\ 9 = rem\frac{17}{9} = 8,$$

$$N_4 = (4 \times 8 + 1)\ mod\ 9 = 33\ mod\ 9 = rem\frac{33}{9} = 6,$$

$$N_{5-10} = 7, 2, 0, 1, 5, 3.$$

We get a sequence of length $M = 9$, after which the entire sequence repeats. If we want numbers in the range [0,1], we divide the N 's by $M = 9$:

0.333, 0.444, 0.889, 0.667, 0.778, 0.222, 0.000, 0.111, 0.555, 0.333.

This is still a sequence of length 9 but is no longer a sequence of integers.

2.4 The Trial Wave Function

The exact wave function is a solution to the Schrodinger equation. Trial wave functions are of central importance in VMC calculations because they introduce importance sampling and control both the statistical efficiency and accuracy obtained. The trial wave function must approximate an exact eigenstate in order that accurate results are to be obtained. A good trial wave function should exhibit much of the same features as does the exact wave function. On one hand, the trial wave function must satisfy some basic conditions [3]:

1) The value of $(\widehat{H}\psi_T(\mathrm{R}))$ must be well defined everywhere. Hence both $\psi_T(\mathrm{R})$ and $\nabla\psi_T(\mathrm{R})$ must be continuous wherever the potential is finite otherwise differentiating will give singular term. One must particularly careful at the edges of the periodic box and when two particles approach

each other. Otherwise, the variational energy E_{VMC} could lie above or below the true energy.

2) The integrals $\int \psi_T^*(\boldsymbol{R})\hat{H}\psi_T(\boldsymbol{R})d$, $\int|\psi_T(\boldsymbol{R})|^2 d\boldsymbol{R}$ and $\int\left|\psi_T(\boldsymbol{R})\hat{H}\right|^2 d\boldsymbol{R}$ must exist. The existence should be demonstrated analytically.

Chapter 3

The Hydrogen Molecule and Its Molecular Ion

3.1 Introduction

Hydrogen is the smallest chemical element because it consists of only one proton in its nucleus and has only one electron. Its chemical symbol is H and its atomic number is 1. It is the lightest element on the periodic table. At standard temperature and pressure hydrogen is a colorless, odorless, tasteless, non-toxic, nonmetallic, highly combustible diatomic gas with the molecular formula H_2. Molecules are systems consisting of electrons and nuclei. Two hydrogen atoms will each share their one electron to form a covalent bond and make a hydrogen molecule H_2. The hydrogen molecular ion H_2^+ can be formed from ionization of a neutral hydrogen molecule. The hydrogen molecular ion H_2^+ is the simplest molecular ion. It consists of two hydrogen nuclei with a single electron. The H_2^+ molecular ion and the H_2 molecule are the two simplest molecular systems whose study has rendered important information in the understanding of the electronic and structural properties of larger molecules and constitute the cornerstones of the actual development of molecular physics.

Alexandr and Coldwell have used widely the variational Monte Carlo method and simple explicitly correlated wave functions at different internuclear distances to calculate molecular energies as well as several energy derivatives at the equilibrium of the hydrogen molecular ion [37]. Also, they have computed the Born-Oppenheimer energy, the spectroscopic constants, the electron density, several of the lowest vibrational-rotational energies of all the hydrogen molecule isotopomers and many properties of

the lowest rovibrational state of all the H_2 isotopomers for the ground state of the hydrogen molecule H_2 [38-42].

Ishikawa *et al.* [43] have solved accurately the nonrelativistic Schrödinger equation and the relativistic four-component Dirac equation of the hydrogen molecular ion H_2^+ in an analytical expansion form by the free iterative complement interaction (ICI) method combined with the variational principle. They calculated both ground and excited states in good convergence, and not only the upper bound but also the lower bound of the ground-state energy. The error bound analysis has assured that their result is highly accurate.

Kurokawa *et al.* [44] has been applied the free ICI method based on the scaled Schrödinger equation proposed previously to the calculations of very accurate wave functions of the hydrogen molecule in an analytical expansion form.

Suleiman *et al.* [45] calculated numerically the ground state energy of hydrogen molecule at different interproton separation under the principles of the Born-Oppenheimer approximation using Monte Carlo technique i.e. the variational Quantum Monte Carlo [VQMC] technique. The results demonstrated that VQMC is capable of approaching the precise ground-state energy of the hydrogen molecule as it falls inside the error bars of previous empirical and numerical calculations.

Our goal in this chapter is to use variational Monte Carlo (VMC) method which introduced in details in the previous chapter to achieve several purposes:

(a) Firstly, in frame of the Born-Oppenheimer (BO) approximation we shall solve Schrödinger equation to calculate the ground state energy of the hydrogen molecular ion H_2^+ and the hydrogen molecule H_2. The

calculations will be done using one trial wave function for the hydrogen molecular ion H_2^+ and two different types of trial wave functions for the hydrogen molecule H_2. Then we will study the accuracy of the results corresponding to each one.

(b) Secondly, to calculate some properties of the hydrogen molecule H_2.

3.2 The Statement of the Problem

In our work, we assume that the nuclear mass is infinite so that the calculations will be in frame of the Born–Oppenheimer approximation. The Hamiltonian function for an arbitrary system (molecule as example) is written in the form:

$$\hat{H} = T + V \tag{3.1}$$

where T is the kinetic energy of the system and V is the potential energy. The potential energy function will contain for the hydrogen molecule terms for the attraction of the electrons to each of the nuclei and a term for the repulsion between the two nuclei as well as the repulsion between the two electrons. Accordingly, the non-relativistic Hamiltonian $\hat{H}$ for the hydrogen molecular system in atomic units (a. u.) can be written as:

$$\hat{H} = -\frac{1}{2}\sum_{i=1}^{2}\nabla_i^2 - \sum_{i=1}^{2}\left(\frac{Z_a}{r_{ia}} + \frac{Z_b}{r_{ib}}\right) + \frac{1}{r_{12}} + \frac{1}{R} \tag{3.2}$$

In the above equation, $r_{ia(b)} = \left|r_{ia(b)}\right|$ denotes the distance from electron 'i' ($i = 1, 2$) to nucleus a (b) and we have used the fact that the charge parameters $Z_a = Z_b = 1$. Also, ∇_i^2 is the Laplacian with respect to the electrons coordinates, r_{12} is the interelectronic distance and R is the internuclear distance. The corresponding coordinates of the two electrons and the two nuclei for the hydrogen molecule are shown in Figure-3.1

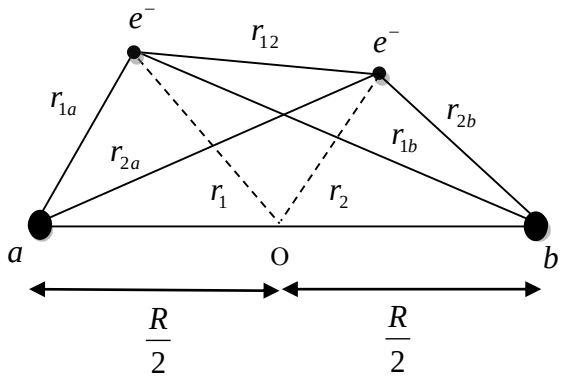

Figure-3.1 Schematic illustration for the hydrogen molecule H_2.

Then, the Schrödinger equation for any trial wave function $\psi(\boldsymbol{r}, \boldsymbol{R})$ can be written as follows

$$\hat{H}\psi(\boldsymbol{r}, R) = E\psi(\boldsymbol{r}, R) \tag{3.3}$$

where $\boldsymbol{r}$ stands for all the coordinate vectors of the electrons with respect to the center of mass of the nuclei.

Similarly in the case of the hydrogen molecular ion H_2^+, if r_a and r_b denote the distances from the electron to the two nuclei *a* and *b*, then the nonrelativistic Hamiltonian operator for the hydrogen molecular ion H_2^+ corresponding to the coordinates of the electron and the two nuclei is given by

$$\hat{H} = -\frac{1}{2}\nabla^2 - \frac{1}{\boldsymbol{r}_a} - \frac{1}{\boldsymbol{r}_b} + \frac{1}{R} \tag{3.4}$$

The corresponding coordinates of the electron and the two nuclei for the hydrogen molecular ion are shown in Figure-3.2

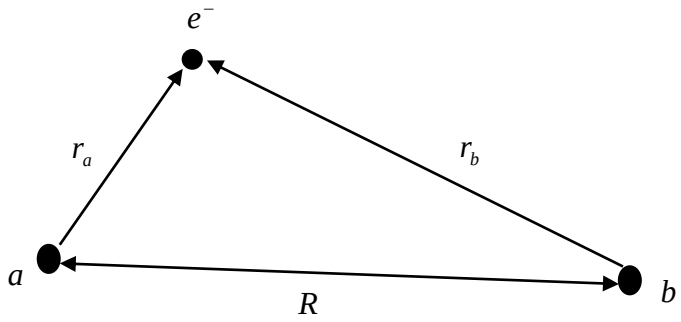

Figure-3.2 Schematic illustration for the hydrogen molecular ion H_2^+.

With a chosen trial wave function ψ explicit expression can be worked out for the local energy $E_L(\boldsymbol{R})$ in terms of the values and derivatives of ψ. In our calculations we have used the nonrelativistic Hamiltonian of the hydrogen molecule, given by Eq. (3.2) in Elliptic Coordinates which take the form [44, 46, 47]

$$\lambda_i = \frac{r_{ia} + r_{ib}}{R}, \qquad \mu_i = \frac{r_{ia} - r_{ib}}{R} \tag{3.5}$$

where i being 1 and 2.

The ranges of these variables are

$$1 \leq \lambda \leq \infty, \qquad -1 \leq \mu \leq 1 \tag{3.6}$$

In these coordinates, the kinetic-energy operator and the potential-energy operator, for the hydrogen molecule, are written as [44, 46, 47]

$$-\frac{1}{2}\nabla_i^2 = -\frac{2}{R^2\left(\lambda_i^2 - \mu_i^2\right)}\left\{\frac{\partial}{\partial\lambda_i}\left(\lambda_i^2 - 1\right)\frac{\partial}{\partial\lambda_i} + \frac{\partial}{\partial\mu_i}\left(1 - \mu_i^2\right)\frac{\partial}{\partial\mu_i}\right\} \tag{3.7}$$

$$V = -\frac{4}{R}\left(\frac{\lambda_1}{\lambda_1^2 - \mu_1^2} + \frac{\lambda_2}{\lambda_2^2 - \mu_2^2} - \frac{1}{2\rho}\right) + \frac{1}{R}, \tag{3.8}$$

respectively, where $\rho = 2r_{12}/R$.

In the calculations of the ground-state energy of the hydrogen molecule we have used the nonrelativistic general Hamiltonian for n-electrons and N_μ-nuclei, which in Hylleraas Coordinates takes the form [48]

$$\widehat{H} = -\sum_{i=1}^{n}\sum_{\mu}^{N_\mu}\left(\frac{1}{2}\frac{\partial^2}{\partial r_{i\mu}^2}+\frac{1}{r_{i\mu}}\frac{\partial}{\partial r_{i\mu}}+\frac{Z_\mu}{r_{i\mu}}\right)-\sum_{i<j}^{n}\left(\frac{1}{2}\frac{\partial^2}{\partial r_{ij}^2}+\frac{1}{r_{ij}}\frac{\partial}{\partial r_{ij}}\right)+$$

$$\sum_{i<j}^{n}\frac{1}{r_{ij}}-\frac{1}{2}\sum_{i=1}^{n}\sum_{\mu<\nu}^{N_\mu}\frac{r_{i\mu}^2+r_{i\nu}^2-r_{\mu\nu}^2}{r_{i\mu}r_{i\nu}}\frac{\partial^2}{\partial r_{i\mu}\,\partial r_{i\nu}}-\frac{1}{2}\sum_{i<j}^{n}\sum_{\mu}^{N_\mu}\frac{r_{i\mu}^2+r_{ij}^2-r_{j\mu}^2}{r_{i\mu}r_{ij}}\frac{\partial^2}{\partial r_{i\mu}\,\partial r_{ij}}-$$

$$\frac{1}{2}\sum_{i<j}^{n}\sum_{j<k}^{n}\frac{r_{ij}^2+r_{ik}^2-r_{jk}^2}{r_{ij}r_{ik}}\frac{\partial^2}{\partial r_{ij}\,\partial r_{ik}}+\sum_{\mu<\nu}^{N_\mu}\frac{Z_\mu Z_\nu}{R_{\mu\nu}}-\frac{1}{2}\sum_{i=1}^{n}\sum_{\mu}^{N_\mu}\frac{1}{r_{i\mu}^2}\frac{\partial^2}{\partial\theta_{i\mu}^2}-$$

$$\frac{1}{2}\sum_{i=1}^{n}\sum_{\mu}^{N_\mu}\frac{cot\theta_{i\mu}}{r_{i\mu}^2}\frac{\partial}{\partial\theta_{i\mu}}-\frac{1}{2}\sum_{i=1}^{n}\sum_{\mu}^{N_\mu}\frac{1}{r_{i\mu}^2 sin^2\theta_{i\mu}}\frac{\partial^2}{\partial\varphi_{i\mu}^2}-$$

$$\frac{1}{2}\sum_{i=1}^{n}\sum_{\mu\neq\nu}^{N_\mu}\left(\frac{1}{2}cot\theta_{i\nu}\frac{r_{i\mu}^2+r_{i\nu}^2-r_{\mu\nu}^2}{r_{i\mu}r_{i\nu}}-\frac{cos\theta_{i\mu}}{r_{i\nu}sin\theta_{i\nu}}\right)\frac{\partial^2}{\partial r_{i\mu}\,\partial\theta_{i\nu}}-$$

$$\sum_{i=1}^{n}\sum_{\mu\neq\nu}^{N_\mu}\frac{sin\theta_{i\mu}}{r_{i\mu}r_{i\nu}sin\theta_{i\nu}}sin\left(\varphi_{i\mu}-\varphi_{i\nu}\right)\frac{\partial^2}{\partial r_{i\mu}\,\partial\varphi_{i\nu}}-$$

$$\sum_{i=1}^{n}\sum_{\mu<\nu}^{N_\mu}\left(\frac{1}{2}cot\theta_{i\mu}cot\theta_{i\nu}\frac{r_{i\mu}^2+r_{i\nu}^2-r_{\mu\nu}^2}{r_{i\mu}^2r_{i\nu}^2}-\frac{cos^2\theta_{i\mu}+cos^2\theta_{i\nu}}{r_{i\mu}\,r_{i\nu}\,sin\theta_{i\mu}\,sin\theta_{i\nu}}\right)\frac{\partial^2}{\partial\theta_{i\mu}\,\partial\theta_{i\nu}}-$$

$$\sum_{i=1}^{n}\sum_{\mu<\nu}^{N_\mu}\frac{cos\left(\theta_{i\mu}-\theta_{i\nu}\right)}{r_{i\mu}r_{i\nu}\,sin\theta_{i\mu}\,sin\theta_{i\nu}}\frac{\partial^2}{\partial\varphi_{i\mu}\,\partial\varphi_{i\nu}}-\sum_{i=1}^{n}\sum_{\mu\neq\nu}^{N_\mu}\frac{cos\theta_{i\mu}}{r_{i\mu}r_{i\nu}sin\theta_{i\nu}}sin\big(\varphi_{i\mu}-$$

$$\varphi_{i\nu}\big)\frac{\partial^2}{\partial\theta_{i\mu}\,\partial\varphi_{i\nu}}-\sum_{i<j}^{n}\sum_{\mu}^{N_\mu}\left(\frac{r_{j\mu}cos\theta_{j\mu}}{r_{ij}r_{i\mu}sin\theta_{i\mu}}+\frac{1}{2}cot\theta_{i\mu}\frac{r_{ij}^2-r_{i\mu}^2-r_{j\mu}^2}{r_{ij}r_{i\mu}}\right)\frac{\partial^2}{\partial\theta_{ij}\,\partial\varphi_{i\mu}}-$$

$$\sum_{i=1}^{n}\sum_{\mu\neq\nu}^{N_\mu}\frac{r_{j\mu}sin\theta_{j\mu}}{r_{ij}r_{i\mu}sin\theta_{i\mu}}sin\left(\varphi_{i\mu}-\varphi_{j\mu}\right)\frac{\partial^2}{\partial r_{ij}\,\partial\varphi_{i\mu}} \tag{3.9}$$

Furthermore, we have used only radial coordinates in the trial wave function so, we omit the spherical terms in Eq. (3.9)

$$\widehat{H} = -\sum_{i=1}^{n}\sum_{\mu}^{N_\mu}\left(\frac{1}{2}\frac{\partial^2}{\partial r_{i\mu}^2}+\frac{1}{r_{i\mu}}\frac{\partial}{\partial r_{i\mu}}+\frac{Z_\mu}{r_{i\mu}}\right)-\sum_{i<j}^{n}\left(\frac{1}{2}\frac{\partial^2}{\partial r_{ij}^2}+\frac{1}{r_{ij}}\frac{\partial}{\partial r_{ij}}\right)+$$

$$\sum_{i<j}^{n}\frac{1}{r_{ij}}-\frac{1}{2}\sum_{i=1}^{n}\sum_{\mu<\nu}^{N_\mu}\frac{r_{i\mu}^2+r_{i\nu}^2-r_{\mu\nu}^2}{r_{i\mu}r_{i\nu}}\frac{\partial^2}{\partial r_{i\mu}\,\partial r_{i\nu}}-\frac{1}{2}\sum_{i<j}^{n}\sum_{\mu}^{N_\mu}\frac{r_{i\mu}^2+r_{ij}^2-r_{j\mu}^2}{r_{i\mu}r_{ij}}\frac{\partial^2}{\partial r_{i\mu}\,\partial r_{ij}}-$$

$$\frac{1}{2}\sum_{i<j}^{n}\sum_{j<k}^{n}\frac{r_{ij}^2+r_{ik}^2-r_{jk}^2}{r_{ij}r_{ik}}\frac{\partial^2}{\partial r_{ij}\,\partial r_{ik}}+\sum_{\mu<\nu}^{N_\mu}\frac{Z_\mu Z_\nu}{R_{\mu\nu}} \tag{3.10}$$

In the case of the hydrogen molecule $n = 2$ (electron 1 and electron 2), $N_\mu = 2$ (nucleus a and nucleus b) and we get

$$\widehat{H} = -\sum_{i=1}^{2}\sum_{\mu=1}^{2}\left(\frac{1}{2}\frac{\partial^2}{\partial r_{i\mu}^2}+\frac{1}{r_{i\mu}}\frac{\partial}{\partial r_{i\mu}}+\frac{Z_\mu}{r_{i\mu}}\right)-\left(\frac{1}{2}\frac{\partial^2}{\partial r_{12}^2}+\frac{1}{r_{12}}\frac{\partial}{\partial r_{12}}\right)+\frac{1}{r_{12}}-$$

$$-\frac{1}{2}\sum_{i=1}^{n}\frac{r_{i1}^2+r_{i2}^2-r_{12}^2}{r_{i1}r_{i2}}\frac{\partial^2}{\partial r_{i1}\,\partial r_{i2}}-\frac{1}{2}\sum_{\mu=1}^{2}\frac{r_{1\mu}^2+r_{12}^2-r_{2\mu}^2}{r_{1\mu}r_{12}}\frac{\partial^2}{\partial r_{1\mu}\,\partial r_{12}}+\frac{1}{R_{12}}. \qquad (3.11)$$

3.3 The Trial Wave Functions

To calculate the ground state energy of the hydrogen molecular ion H_2^+ and the hydrogen molecule H_2, we will use different types of trial wave functions. The trial wave function for the ground state of the hydrogen molecular ion H_2^+ used in this work is given by Ishikawa *et al.* [43]. This trial wave function depends on the Slater type function ψ_0 as initial function which takes the form:

$$\psi_0 = exp(-\omega\lambda) \qquad (3.12)$$

where ω is nonlinear parameter. In this choice, the trial wave function ψ_1 is generated in the analytical expansion form of

$$\psi_1 = \sum_i C_i\,\lambda^{m_i}\,\mu^{n_i}\,exp(-\omega\lambda), \qquad (3.13)$$

where C_i are the variational parameters and m_i are positive or negative integers. Since the $1s\sigma_g$ ground-state has a gerade symmetry, n_i should be zero or a positive even integer. Applying the iterative complement interaction (ICI) method, Ishikawa *et al.* [43] used this trial wave function to calculate energies for the ground-state $1s\sigma_g$ of H_2^+ at different orders and the first excited state $1s\sigma_u$ (ungerade) in the free case. They could obtain very accurate results compared to the corresponding exact values.

For the ground state, the overlap and Hamiltonian integrals of H_2^+ are easily done when the wave function is given by Eq. (3.13).

This wave function (3.13) constructed from 26 terms for the H_2^+ with $\omega = 1.2$. We show this terms in Table-3.1.

Table-3.1 The values of the parameters m, n and C appearing in the wave function ψ_1 of Eq (3.13) and $\omega = 1.2$ [43].

No.	m	n	C	No.	m	n	C
1	1	2	-6.14854851224062E-04	14	-4	0	-7.44380959774439E-03
2	1	0	-8.72134862233988E-04	15	-4	2	-1.10143056220481E-02
3	-3	4	6.49330072561502E-02	16	-2	4	-3.45048628383914E-02
4	-4	4	-3.96590873312382E-02	17	0	2	1.46302680608681E-02
5	-1	4	1.52822020322079E-03	18	-5	2	1.08079860246917E-02
6	0	0	2.44061495121818E-02	19	-6	2	1.73761624309944E-01
7	-2	0	-5.74894612410661E-02	20	-5	0	4.63828712981874E-03
8	-3	0	5.49994904166429E-02	21	-6	0	-4.09990053189853E-02
9	-2	2	1.99545888257851E-01	22	-7	0	2.61468592559640E-02
10	-3	2	-2.16145726972879E-01	23	-7	2	-1.15084145925041E-01
11	2	0	-7.85025721800686E-04	24	-3	6	-1.11401171197032E-03
12	-1	0	2.78206161933570E-02	25	-5	4	1.57204422348785E-02
13	-1	2	-4.88622788195747E-02	26	3	0	7.58881756418373E-05

In the case of the hydrogen molecule H_2 we will use two different types of trial wave functions:

1- The first type for the ground state of H_2 molecule, this wave function is proposed firstly by Kurokawa *et al.* [44]. This trial wave function depends on the Slater type functions which takes the form:

$$\psi_2 = \sum_i C_i(1 + p_{12})\, exp[-\alpha(\lambda_1 + \lambda_2)]\ \lambda_1^{m_i}\, \lambda_2^{n_i}\, \mu_1^{j_i}\, \mu_2^{k_i}\, \rho^{l_i}, \qquad (3.14)$$

where p_{12} is an electron exchange operator and C_i are the variational parameters which are calculated from the variational principle. This wave function is very simple and similar to the original wave function due to James and Coolidge [49]. James-Coolidge wave function and this wave function differ only in the powers m_i and n_i of the variables λ_1 and λ_2: m_i

and n_i are always positive in the James-Coolidge wave function, but they can be even negative in this free wave function.

This wave function was constructed from 13 terms; 11 terms of James and Coolidge plus 2 terms within the range of $-1 \leq m,n \leq 1$, $|m-n| \leq 1$, $j \geq 0$, $k \leq 2$, $0 \leq l \leq 1$. The term No. 12 has positive m and n, but the term No. 13 has negative m and n. This wave function was used with iterative-complement-interaction (ICI) method to calculate the ground state energy of free hydrogen molecule [44]. We show the 13 terms of ψ_2 in Table-3.2 with $\alpha = \frac{3}{4}$.

Table-3.2 The values of the parameters m, n, j, k, l and C for the wave function ψ_2 of Eq. (3.14) with $\alpha = \frac{3}{4}$ [44].

No.	m	n	j	k	l	C
1	0	0	0	0	0	1.000 000 000
2	0	0	0	0	1	0.650 858 318
3	0	0	0	0	2	−0.059 439 543
4	0	0	0	2	0	0.138 956 703
5	0	0	1	1	0	−0.041 545 078
6	1	0	0	0	0	−0.933 425 960
7	1	0	0	2	0	−0.018 305 773
8	1	0	1	1	0	0.015 613 455
9	1	0	2	0	0	−0.033 975 753
10	1	0	0	0	1	−0.404 443 002
11	2	0	0	0	0	0.337 386 255
12	1	1	0	0	1	0.071 193 197
13	-1	-1	0	2	1	0.031 686 115

2-The second type of trial wave function of H_2 molecule is a product of three items which takes the form [45]:

$$\psi_3(r_1, r_2, r_{12}) = \varphi(r_1)\varphi(r_2)f(r_{12}) \tag{3.15}$$

where $\varphi(r_i)$ is the single-particle wave function for particle i, and $f(r_{12})$ accounts for more complicated two-body correlations.

Here, the first two factors are independent-particle wave functions, their roles are to place each electron in a molecular orbital in which it is shared equally between the two protons. A good choice for the molecular orbital is the symmetric linear combination of atomic orbitals centered about each proton,

A suitable choose for the trial wave function arises from the fact that two electrons are in $1s$ state to calculate the ground state. A simple choice for $\varphi(r_i)$ is:

$$\varphi(r_i) = exp\left(-\dot{Z}\ r_{ia}\right) + exp\left(-\dot{Z}\ r_{ib}\right), \tag{3.16}$$

with the variational parameter $\dot{Z}$ to be determined. The final factor in the trial wave function f expresses the correlation between the two electrons due to their Coulomb repulsion. That is, we expect f to be small when r_{12} is small and to approach a large constant value as the electrons become well separated. A convenient and reasonable choice is

$$f(r) = exp\left[\frac{r}{\alpha(1+\beta r)}\right], \tag{3.17}$$

where α and β are additional positive variational parameters. The variational parameter β controls the distance over which the trial wave function heals to its uncorrelated value as the two electrons separate.

Then putting (3.16), (3.17) in (3.15) a collection of a justifiable trial wave function is attained:

$$\psi_3(r_1, r_2, r_{12}) = \left[exp\left(-\dot{Z}\ r_{1a}\right) + exp\left(-\dot{Z}\ r_{1b}\right)\right]\left[exp\left(-\dot{Z}\ r_{2a}\right) + exp\left(-\dot{Z}\ r_{2b}\right)\right]exp\left[\frac{r_{12}}{\alpha(1+\beta r_{12})}\right] \tag{3.18}$$

The singularity of the coulomb potential at short distances places additional constraints on the trial wave function. If one electron approaches the nuclei while the other electron remains fixed then the potential term becomes large

and negative, since $r_{ia(b)}$ becomes small. This must be cancelled by a corresponding positive divergence in the kinetic energy term if we are to keep the local energy E_L smooth variance in the Monte Carlo quadrature. Thus the orbital $\varphi(r_i)$ should a cusp at $r_{ia(b)} = 0$, which means that the wave function should satisfy the following relation [45]:

$$\lim_{r_{ia(b)}\to 0}\left(-\frac{1}{\varphi(r_i)}\nabla_i^2\varphi(r_i) - \frac{1}{r_{ia(b)}}\right) = finite\ terms. \tag{3.19}$$

The above relation holds for $r_{1a}, r_{1b}, r_{2a}, r_{2b}$ and also for r_{12}. Using Eq. (3.19) and a bit of algebra, it is easy to see that these constraints imply that α satisfies the transcendental equation:

$$\alpha = \frac{1}{1+e^{-R/a}} \tag{3.20}$$

and that $\alpha = 2\ a_0$, where $a_0 = \frac{\hbar^2}{me^2}$ is the Bohr radius i.e. $\alpha = 2$ in atomic units. Thus β is the only variational parameter at our disposal.

3.4 Discussion of the Results of Chapter 3

In this chapter we have used VMC method which presented in Chapter 2 to calculate both the ground state energies of the hydrogen molecular ion H_2^+ and the hydrogen molecule H_2 and also some properties of the hydrogen molecule H_2. All energies obtained in atomic units i.e. ($\hbar = e = m_e = 1$) with a set of 4×10^7 Monte Carlo integration points in order to make the statistical error as small as possible. This section presents the results obtained with different types of the trial wave functions for the H_2 molecule proposed in the previous section.

In frame of the Born-Oppenheimer (BO) approximation, the ground state energies of the hydrogen molecular ion H_2^+ and the hydrogen molecule H_2

were calculated using VMC method. For the ground state, our calculations are based on using different types of trial wave functions.

On the first hand to gain some confidence on the adequacy of different types trial wave functions given by Eq. (3.13), Eq. (3.14) and Eq. (3.18) for our calculations in frame of VMC method, we first calculate the ground state energy in the case of free hydrogen molecular ion H_2^+ for different values of the internuclear distance R. We have used the nonrelativistic Hamiltonian given by Eq. (3.5) using ψ_1 in Elliptic Coordinates.

In Table-3.3 we compare the results of our work for the behavior of the total energy of the ground-state $(1s\sigma_g)$ of free H_2^+ ion at different values for the internuclear distance R with the exact calculations by Madsen *et al*. [50] and other accurate calculations by Zhang *et al*. [51]. Excellent quantitative agreement is obtained compared to the corresponding exact values and other previous results.

The results of accurate calculations of the electronic ground-state $(1s\sigma_g)$ energy of H_2^+ with $R = 2.0$ a.u. are summarized in Table-3.4. We report the results obtained in Table-3.4 here as the electronic energy where the total electronic energy of the molecular ion H_2^+ is defined as the total energy E_T minus the repulsive energy between the nuclei, $E_{ele} = E_T - \frac{Z_a Z_b}{R}$. We show the ground state energy in the Born-Oppenheimer approximation to compare our results with the results of previous authors and we got good agreement.

Table-3.3 Total energy of the free H_2^+ ion for the trial wave function ψ_1 for various internuclear distance *R* compared with the exact values by Madsen *et al*. [50] and other accurate calculations by Zhang *et al*. [51]. In parentheses, we show the statistical error in the last figure.

R	$E_{This\ work}$	E^a	E_{Exact}
1	-0.451590(2)	-	-0.4517863133781[b]
2	-0.602634(5)	−0.60263414	-0.6026342145[b]
3	-0.57749866(3)	-	-0.577562864[b]
4	-0.79594490(2)	−0.79608445	−0.79608488[c]
6	-0.67821670(6)	−0.67863445	−0.67863572[c]
8	-0.626574200(3)	−0.62756682	−0.62757039[c]
10	-0.600191600(2)	−0.60057303	−0.60057873[c]

[a] Ref [51] [b] Ref [50] [c] The exact Results taken from Ref [51]

Table-3.4 History of accurate calculations of the electronic energy of H_2^+ with $R = 2.0$ a.u.

The Type	References	Total energy (a.u.)
Exact wave function[a]	J. M. Peek	−1.102 634 214 494 9
ICI method[b]	Atsushi Ishikawa - Hiroyuki Nakashima - Hiroshi Nakatsuji	−1.102 634 20
Correlated wave function[c]	F. Weinhold - A. B. Chinen	−1.102 623 7
Finite element method[d]	W. Schulze - D. Kolb	−1.102 632 7
Finite difference method[e]	L. Laaksonen - P. Pyykko - D. Sundholm	−1.102 634 214 497
VMC method	Present	-1.102 634 0

[a] Ref [52] [b] Ref [43] [c] Ref [53] [d] Ref [54] [e] Ref [55]

Secondly, we calculate the ground state energy in the case of free hydrogen H_2 molecule using ψ_2 and ψ_3 for different values of the internuclear distance R. We have used the nonrelativistic Hamiltonian given by Eq. (3.4) using ψ_2 in Elliptic Coordinates and ψ_3 in Hylleraas Coordinates. In Table-3.5 we compare the results of our work for the behavior of the total energy of the ground state of free H_2 molecule with other pervious calculations for a wide set of internuclear distances. For internuclear distances in the range $0.6 \leq R \leq 3.2$ it was sufficient to compare our values with the available single-configuration Hartree–Fock SCF in Ref [56], whereas for $4.0 \leq R \leq 8.0$ we compare with results of Ref [57]. Also, the results obtained by Rodriguez *et al*. [46] are introduced. The results presented in Table-3.5 indicate clearly that when R increases the interaction between the electrons become less and less, particularly around the nuclei. Each nucleus has an electron and the probability for both being around the same nucleus is small, as one would expect. When R increases, the H_2 molecule tends to separate to two hydrogen atoms in their ground state therefore the ground state energy decreases. A good quantitative agreement is obtained using ψ_2 and ψ_3 compared to the corresponding accurate values.

Table-3.5 Ground-state energy of the free H_2 molecule as function of the internuclear distance. In parentheses, we show the statistical error in the last figure.

R	ψ_2	ψ_3	E_{SCF}	E^c
0.2	2.2474800(1)	2.233774(7)	-	2.2478
0.4	-0.0749825(1)	-0.075675(1)	-0.078 693[a]	-0.0756
0.6	-0.7247206(1)	-0.727725(3)	-0.729990[a]	-0.7278
1.0	-1.084500(1)	-1.085004(1)	-1.085138[a]	-1.0843
1.2	-1.124541(2)	-1.124815(2)	-1.125029[a]	-1.1244
1.3	-1.131293(1)	-1.131506(2)	-1.132024[a]	-1.1315
1.35	-1.135239(4)	-1.132803(2)	-	-1.1329
1.375	-1.133103(1)	-1.133636(2)	-1.133642[a]	-1.133(180)
1.4	-1.137474(9)	-1.133509(2)	-1.133630[a]	-1.133(181)
1.425	-1.134544(5)	-1.133294(1)	-1.133379[a]	-1.1329
1.45	-1.136994(5)	-1.132784(1)	-1.132908[a]	-1.1325
1.5	-1.130748(5)	-1.131130(1)	-1.131375[a]	-1.1310
1.6	-1.125689(5)	-1.128542(8)	-1.126352[a]	-1.1259
2.0	-1.091085(1)	-1.087710(9)	-1.091648[a]	-1.0911
2.4	-1.044736(3)	-1.049354(8)	-1.049331[a]	-1.0488
3.2	-0.978582(7)	-0.970015(1)	-0.971512[a]	-0.9704
4.0	-0.916097(6)	-0.900654(4)	-0.909130[b]	-0.9102
6.0	-0.8208544(7)	-0.818213(4)	-0.819032[b]	-0.8214
8.0	-0.7850081(1)	-0.778321(5)	-0.779582[b]	-0.7827

[a] Ref [56]. [b] Ref [57]. [c] Ref [46].

It is interesting to compare the ground state energy for the hydrogen molecular ion, H_2^+, and the hydrogen molecule, H_2. Note that the ground state energy of the H_2 molecule is lower than that of the H_2^+ ion as shown in Table-3.3 and Table-3.5. This should make sense, since in order to get H_2^+ from H_2 we need to ionize the molecule, which takes substantial energy. We note also that the H_2 molecule is stabler than the H_2^+ molecular ion. Finally, we note that when we break the bond we get different products. When we break apart the H_2, we get two H atoms. When we break apart H_2^+, we get H atom and a proton. The difference in energy between the two sets of products is the ionization energy of the H atom.

Finally, using VMC techniques we have computed 13 molecular properties of hydrogen molecule H_2 at 24 internuclear distances. Here the permanent quadrupole moment is defined as $Q_2 = (R^2 + r_{1a}^2 - 3z_1^2 + r_{2a}^2 - 3z_2^2)/2$ and the permanent hexadecapole moment is defined as $Q_4 = (R^4 + 30\, r_{1a}^2 z_1^2 - 35\, z_1^4 - 3\, r_{1a}^4 + 30\, r_{2a}^2 z_2^2 - 35\, z_2^4 - 3\, r_{2a}^4)/8$ for a molecule oriented along the z-axis. As Tables-3.6 to 3.18 show, almost all of our properties are determined to several significant digits. Many of these properties have been calculated using other theoretical methods [58, 59]. We compare our values with Alexandr *et al.* [60]. Our values are in excellent agreement with these earlier results.

In Tables-3.6 to 3.18 we present selected values for the different internuclear distances R for the H_2 molecule. Previous results are also given in these tables.

Table-3.6 Values for $\langle r_{1a} \rangle$ of the hydrogen molecule for selected values of R

R	Present Work	Ref [60]
0.2	1.5876	1.5880
0.4	1.4281	1.4279
0.6	1.2819	1.2820
0.8	1.1615	1.1605
1.0	1.0604	1.0612
1.2	0.9802	0.9800
1.4	0.9134	0.9128
1.6	0.8548	0.8569
1.8	0.8111	0.8103
2.0	0.7710	0.7712
2.2	0.7381	0.7385
2.4	0.7118	0.7112
2.6	0.6885	0.6886
2.8	0.6706	0.6700
3.0	0.6558	0.6548
3.5	0.6293	0.6288
4.0	0.6177	0.6136
4.5	0.6042	0.6035
5.0	0.5951	0.5954
6.0	0.5821	0.5819
7.0	0.5716	0.5707
8.0	0.5625	0.5621
9.0	0.5558	0.5553
10.0	0.5494	0.5498

Table-3.7 Values for $\langle r_{1a}^{-1} \rangle$ of the hydrogen molecule for selected values of R.

R	Present Work	Ref [60]
0.2	0.9670	0.9663
0.4	1.0421	1.0424
0.6	1.1341	1.1348
0.8	1.2346	1.2346
1.0	1.3379	1.3380
1.2	1.4426	1.4430
1.4	1.5480	1.5488
1.6	1.6556	1.6545
1.8	1.7590	1.7598
2.0	1.8647	1.8646
2.2	1.9671	1.9684
2.4	2.0718	2.0710
2.6	2.1758	2.1730
2.8	2.2731	2.2737
3.0	2.3701	2.3735
3.5	2.6121	2.619
4.0	2.8623	2.863
4.5	3.1032	3.104
5.0	3.3486	3.346
6.0	3.8257	3.832
7.0	4.3126	4.322
8.0	4.8177	4.812
9.0	5.2992	5.305
10.0	5.7289	5.799

Table-3.8 Values for $\langle r_{1a}\ r_{1b}\rangle$ of the hydrogen molecule for selected values of R

R	Present Work	Ref [60]
0.2	1.2721	1.2716
0.4	1.4352	1.4360
0.6	1.6448	1.6445
0.8	1.8828	1.8813
1.0	2.1426	2.140
1.2	2.4154	2.4146
1.4	2.7048	2.705
1.6	3.0015	3.005
1.8	3.3169	3.315
2.0	3.6358	3.632
2.2	3.9498	3.951
2.4	4.2766	4.270
2.6	4.5989	4.590
2.8	4.9077	4.904
3.0	5.2118	5.214
3.5	5.9533	5.955
4.0	6.6682	6.662
4.5	7.3470	7.348
5.0	8.0388	8.035
6.0	9.4375	9.433
7.0	10.8649	10.868
8.0	12.3251	12.320
9.0	13.7760	13.778
10.0	15.2511	15.250

Table-3.9 Values for the interelectron distances $\langle r_{12} \rangle$ of the hydrogen molecule for selected values of R

R	Present Work	Ref [60]
0.2	1.4690	1.4697
0.4	1.5650	1.5647
0.6	1.6733	1.6766
0.8	1.7957	1.7956
1.0	1.9175	1.9180
1.2	2.0434	2.0423
1.4	2.1696	2.1692
1.6	2.2998	2.2981
1.8	2.4308	2.4303
2.0	2.5685	2.5671
2.2	2.7099	2.7089
2.4	2.8592	2.8571
2.6	3.0155	3.013
2.8	3.1725	3.178
3.0	3.3549	3.352
3.5	3.8207	3.823
4.0	4.3264	4.327
4.5	4.8362	4.838
5.0	5.3497	5.340
6.0	6.3182	6.318
7.0	7.2804	7.283
8.0	8.2560	8.250
9.0	9.2247	9.222
10.0	10.2031	10.200

Table-3.10 Values for $\langle r_{12}^2 \rangle$ of the hydrogen molecule for selected values of R.

R	Present Work	Ref [60]
0.2	2.6776	2.6798
0.4	3.0207	3.0202
0.6	3.4464	3.447
0.8	3.9265	3.929
1.0	4.4506	4.456
1.2	5.0240	5.023
1.4	5.6326	5.635
1.6	6.2796	6.289
1.8	6.9906	6.995
2.0	7.7698	7.762
2.2	8.5925	8.594
2.4	9.5002	9.503
2.6	10.5080	10.505
2.8	11.6057	11.607
3.0	12.8229	12.820
3.5	16.3675	16.362
4.0	20.5622	20.572
4.5	25.2987	25.29
5.0	30.3845	30.41
6.0	41.8144	41.81
7.0	54.9676	54.95
8.0	69.9512	69.99
9.0	86.9610	86.99
10.0	105.9670	105.99

Table-3.11 Values for $\langle r_{12}^{-1} \rangle$ of the hydrogen molecule for selected values of R.

R	Present Work	Ref [60]
0.2	0.9109	0.9109
0.4	0.8486	0.8484
0.6	0.7834	0.7847
0.8	0.7264	0.7264
1.0	0.6736	0.6744
1.2	0.6281	0.6285
1.4	0.5869	0.5874
1.6	0.5502	0.5506
1.8	0.5181	0.5171
2.0	0.4869	0.4863
2.2	0.4570	0.4577
2.4	0.4309	0.4309
2.6	0.4057	0.4055
2.8	0.3815	0.3814
3.0	0.3583	0.3584
3.5	0.3060	0.3063
4.0	0.2631	0.2630
4.5	0.2291	0.22911
5.0	0.2032	0.20326
6.0	0.1671	0.16719
7.0	0.1428	0.14287
8.0	0.1249	0.12497
9.0	0.1110	0.11109
10.0	0.0999	0.09999

Table-3.12 Values for $\langle r_{1a}^2 \rangle$ of the hydrogen molecule for selected values of R.

R	Present Work	Ref [60]
0.2	1.2778	1.2782
0.4	1.4622	1.4622
0.6	1.7031	1.7031
0.8	1.9860	1.9857
1.0	2.3044	2.304
1.2	2.6559	2.654
1.4	3.0371	3.037
1.6	3.4480	3.447
1.8	3.8870	3.888
2.0	4.3588	4.359
2.2	4.8595	4.857
2.4	5.3869	5.384
2.6	5.9423	5.943
2.8	6.5317	6.533
3.0	7.1552	7.156
3.5	8.8644	8.865
4.0	10.8168	10.812
4.5	12.9985	12.995
5.0	15.4248	15.414
6.0	20.9736	20.96
7.0	27.4091	27.49
8.0	34.9249	34.98
9.0	43.4117	43.48
10.0	52.8949	52.98

Table-3.13 Values for $\langle r_{1a}\ r_{2a} \rangle$ of the hydrogen molecule for selected values of R.

R	Present Work	Ref [60]
0.2	0.8952	0.8959
0.4	1.0461	1.0465
0.6	1.2421	1.2441
0.8	1.4730	1.4757
1.0	1.7345	1.7351
1.2	2.0161	2.0180
1.4	2.3211	2.3221
1.6	2.6410	2.6425
1.8	2.9760	2.977
2.0	3.3265	3.323
2.2	3.6704	3.675
2.4	4.0290	4.028
2.6	4.3787	4.380
2.8	4.7271	4.726
3.0	5.0632	5.061
3.5	5.8430	5.842
4.0	6.5556	6.551
4.5	7.2211	7.222
5.0	7.8981	7.896
6.0	9.2884	9.286
7.0	10.7254	10.728
8.0	12.2032	12.197
9.0	13.6742	13.670
10.0	15.1449	15.153

Table-3.14 Values for $\langle r_{1a}\ r_{2b}\rangle$ of the hydrogen molecule for selected values of R.

R	Present Work	Ref [60]
0.2	0.8971	0.8964
0.4	1.0486	1.0485
0.6	1.2498	1.2497
0.8	1.4852	1.4877
1.0	1.7593	1.7578
1.2	2.0589	2.0570
1.4	2.3828	2.3855
1.6	2.7438	2.7417
1.8	3.1291	3.127
2.0	3.5443	3.543
2.2	3.9907	3.990
2.4	4.4706	4.470
2.6	4.9819	4.987
2.8	5.5413	5.543
3.0	6.1443	6.142
3.5	7.8356	7.833
4.0	9.8121	9.806
4.5	12.0361	12.032
5.0	14.4880	14.488
6.0	20.0310	20.08
7.0	26.6472	26.62
8.0	34.1596	34.12
9.0	42.7169	42.62
10.0	52.1086	52.12

Table-3.15 Values for $\langle x_1\ x_2 \rangle$ of the hydrogen molecule for selected values of R.

R	Present Work	Ref [60]
0.2	-0.0230	-0.02348
0.4	-0.0268	-0.0278
0.6	-0.0333	-0.0329
0.8	-0.0380	-0.0383
1.0	-0.0449	-0.0440
1.2	-0.0485	-0.0498
1.4	-0.0551	-0.0550
1.6	-0.0600	-0.0600
1.8	-0.0640	-0.0635
2.0	-0.0661	-0.0663
2.2	-0.0690	-0.0682
2.4	-0.0680	-0.0689
2.6	-0.0689	-0.0682
2.8	-0.0662	-0.0663
3.0	-0.0630	-0.0631
3.5	-0.0503	-0.0519
4.0	-0.0386	-0.0383
4.5	-0.0274	-0.0271
5.0	-0.0190	-0.0190
6.0	-0.0108	-0.0101
7.0	-0.0056	-0.0053
8.0	-0.0032	-0.0036
9.0	-0.0025	-0.0027
10.0	-0.0017	-0.0019

Table-3.16 Values for $\langle z_1\ z_2 \rangle$ of the hydrogen molecule for selected values of R

R	Present Work	Ref [60]
0.2	-0.0244	-0.02458
0.4	-0.0317	-0.0321
0.6	-0.0440	-0.0441
0.8	-0.0616	-0.0613
1.0	-0.0842	-0.0850
1.2	-0.1169	-0.1167
1.4	-0.1612	-0.1600
1.6	-0.2169	-0.2172
1.8	-0.2926	-0.2919
2.0	-0.3891	-0.3887
2.2	-0.5125	-0.5124
2.4	-0.6686	-0.6685
2.6	-0.8613	-0.8612
2.8	-1.0976	-1.0961
3.0	-1.3771	-1.3758
3.5	-2.2731	-2.271
4.0	-3.3974	-3.394
4.5	-4.6556	-4.655
5.0	-5.9911	-5.996
6.0	-8.7603	-8.9123
7.0	-12.2167	-12.220
8.0	-15.9881	-15.99
9.0	-20.2145	-20.24
10.0	-24.9899	-24.99

Table-3.17 Values for $\langle Q_2 \rangle$ of the hydrogen molecule for selected values of R.

R	Present Work	Ref [60]
0.2	0.0114	0.0114
0.4	0.0452	0.0451
0.6	0.0990	0.0991
0.8	0.1713	0.1706
1.0	0.2558	0.2564
1.2	0.3517	0.3538
1.4	0.4561	0.4563
1.6	0.5641	0.5638
1.8	0.6627	0.6699
2.0	0.7621	0.7689
2.2	0.8574	0.858
2.4	0.9337	0.931
2.6	0.9804	0.985
2.8	1.0144	1.013
3.0	1.0119	1.015
3.5	0.9185	0.905
4.0	0.6972	0.689
4.5	0.4540	0.464
5.0	0.2893	0.287
6.0	0.0734	0.094
7.0	0.0279	0.026
8.0	0.0463	0.008
9.0	0.0036	0.004
10.0	0.0029	0.003

Table-3.18 Values for $\langle Q_4 \rangle$ of the hydrogen molecule for selected values of R.

R	Present Work	Ref [60]
0.2	0.0012	0.001
0.4	0.0047	0.004
0.6	0.0111	0.011
0.8	0.0361	0.036
1.0	0.0829	0.082
1.2	0.1586	0.159
1.4	0.2845	0.281
1.6	0.4577	0.453
1.8	0.6821	0.680
2.0	0.9684	0.968
2.2	1.3057	1.309
2.4	1.6941	1.70
2.6	2.1240	2.10
2.8	2.5050	2.51
3.0	2.9124	2.89
3.5	3.4742	3.48
4.0	3.4336	3.47
4.5	2.9993	2.98
5.0	2.4406	2.29
6.0	1.3816	1.09
7.0	0.5744	0.3
8.0	0.1011	0.1
9.0	0.2103	0.2
10.0	0.2100	0.2

3.5 Conclusion

In this chapter we have used the Variational Monte Carlo method to calculate the ground state energies of the hydrogen molecular ion H_2^+ and the hydrogen molecule H_2 at different internuclear separation. The calculations were carried out numerically under the principles of Born-Oppenheimer approximation which deal with the case of an "infinitely heavy" nucleus. Also, we calculated 13 molecular properties of hydrogen molecule H_2 at 24 internuclear distances. The calculations were based on using different types of trial wave functions. The trial wave functions ψ_1, ψ_2 and ψ_3 are compact and accurate. The obtained results were in good agreement with the corresponding exact and accurate results. Finally, our conclusion is that the variational Monte Carlo method provides accurate estimations for the ground state energy of the two atoms molecules.

Chapter 4

Ground State Calculations of the Confined Hydrogen Molecule H_2, Molecular Ions H_2^+ and HeH^{++} Using Variational Monte Carlo Method

4.1 Introduction

Recently, many studies concerning the problem of confined molecular systems have attracted the attention of both physicists and quantum chemists. This is due to the unusual physical and chemical properties observed in such systems when submitted to narrow spatial limitation as compared to their free cases. When atoms and molecules are confined in either penetrable or impenetrable boundaries their properties undergo significant changes. Also, confined systems are widely used to model a variety of problems in physics and chemistry. For example, the study of the synthesis of nanostructure materials such as carbon nanotubes [61], buckyballs and zeolitic nanochannels which serve as ideal containers for molecular insertion and storage with promising applications [62, 63].

The increasing pace at which research is being carried out in the aforementioned systems demands many powerful and sophisticated methodologies (Hartree–Fock, quantum chemical density functional theory, quantum molecular dynamics, to mention a few [61, 62]) and also, complementary exploratory models aimed at understanding the basic mechanisms of the changes in the electronic and structural properties of a confined molecules. Various theoretical models have been proposed in the

past to analyze confinement effects on the confined systems, particularly those based on boxed-in molecules.

Box models of confinement with hard and soft boundaries have been widely used to survey the effect of spatial limitation in the case of simple molecules such as H_2^+ molecular ion, H_2 molecule and some small polyatomics as H_2O, CH_4, NH_3 and LiF. Since, the H_2^+ molecular ion is considered as one of the first non-trivial quantum mechanical systems, many studies have been presented recently to investigate it under compression.

In Ref [64], Molinar-Tabares *et al.* studied the H_2^+ confined by spheroids of size ξ_0 using prolate spheroidal coordinates. In frame of Born–Oppenheimer approximation, the Schrödinger equation was solved by the method of separation of variables to obtain the equilibrium distance between nuclei and the corresponding energy as functions of ξ_0. Also, the vibrational energy of the nuclei, the pressure, the polarizability and the anisotropy were calculated.

A first successful attempt to uncouple the nuclear positions from the foci was made by Crus *et al*. [65] for H_2^+ confined within impenetrable prolate spheroidal boxes. The non-separable Schrödinger problem was solved using the variational method with simple LCAO Dickinson type variational ansatz wave function to obtain the ground state energies of the enclosed H_2^+ and HeH^{++} when the nuclear positions do not coincide with the foci. The pervious results were extended to cover case of H_2 by Rodriguez *et al*. [46]. They considered the case of the H_2 molecule confined by impenetrable spheroidal boxes when the nuclei do not coincide with the foci. It was shown that by making the cavity size and shape independent of the nuclear positions, optimum equilibrium bond lengths and energies are obtained as

compared with corresponding on-focus calculations. This procedure allows for a controlled treatment of molecular properties by selecting an arbitrary size and shape of the confining spheroidal box.

In Ref [47], a generalization of previous theoretical studies of molecular confinement based on the molecule-in-a-box model was presented. In contrast with previous box models of molecular confinement, this work introduced a new treatment allows for full control of cavity size and shape, internuclear positions and confining barrier height. The presented model adds more flexibility for dealing with the electronic and vibrational properties of electrons under compression which lead to more realistic comparison with experiment. Also, this study shows that as the cavity size is reduced, the limit of stability of the confined molecule is attained for a critical size.

One of the most and recent studies was presented by Sarsa *et al.* [66] where the H_2^+ molecular ion confined by impenetrable spherical surfaces was studied beyond the Born–Oppenheimer approximation. The confinement of both electron and nuclei were considered and they could show that the electron constraint is much more efficient to increase the energy than the nuclei confinement.

4.2 Description of the Problem

In this chapter we have studied the ground state energy of H_2^+ molecular ion and H_2 molecule confined by a hard prolate spheroidal cavity under compression effects using variational Monte Carlo method. Our results were extended also to include the HeH^{++} molecular ion.

We considered the H_2 molecule and the H_2^+ molecular ion confined within a prolate spheroidal cavity, defined by the geometric contour ξ_0 as shown in

Figure-4.1 and Figure-4.2. Then, the Schrödinger equation for the confined molecules can be written as follows

$$\left(\widehat{H} - E\right)\psi = 0, \tag{4.1}$$

The Hamiltonian function in equation (4.1) is written in the form:

$$\widehat{H} = T + V \tag{4.2}$$

In equation (4.2) the kinetic energy $T = -\frac{1}{2}\sum_{i=1}^{n} \nabla_i^2$ is the sum of the kinetic energies of the two electrons and ∇_i^2 is the Laplacian with respect to the coordinates of the electron i. The potential energy V is the total potential energy of the system.

Considering the origin is placed at the center of mass of the nuclei then the total potential energy of the confined hydrogen molecular system in atomic units (a. u.) can be written as:

$$V = -\sum_{i=1}^{n}\left(\frac{1}{r_{ia}} + \frac{1}{r_{ib}}\right) + \frac{1}{r_{12}} + \frac{1}{R} + V_c \tag{4.3}$$

In the above equation, $r_{ia(b)} = \left|\boldsymbol{r}_{ia(b)}\right|$ denotes the distance from electron 'i' $(i = 1, 2)$ to nucleus 'a' ('b'), r_{12} is the interelectronic distance and R is the internuclear distance. The index n runs over the numbers of the electrons so that for the hydrogen molecule $n = 2$. For the hydrogen molecular ion H_2^+ the index $n = 1$.

The potential V_c is the confining barrier imposed by the spheroidal boundary (S), which is infinitely high when the electron or one nucleus is at the respective defined boundary surfaces—spheroidal or spherical—and equals zero when the particles are inside the volume limited by the surfaces, that is

$$V_c = \begin{cases} \infty & (r_{ia}, r_{ib}) \in S \\ 0 & (r_{ia}, r_{ib}) \notin S \end{cases} \tag{4.4}$$

From equation (4.3), at $n = 1$ the molecular Hamiltonian for the confined H_2^+ molecular ion may be conveniently written (in atomic units) as follows [66]

$$\widehat{H} = -\frac{1}{2}\nabla^2 - \frac{1}{r_a} - \frac{1}{r_b} + \frac{1}{R} + V_c. \tag{4.5}$$

In the above equation, r_a and r_b denote the distances from the electron to nuclei a, b

$$r_a = \sqrt{x^2 + y^2 + \left(z + \tfrac{1}{2}R\right)^2}, \quad r_b = \sqrt{x^2 + y^2 + \left(z - \tfrac{1}{2}R\right)^2}, \tag{4.6}$$

From equation (4.3), at $n = 2$ it was easy to write down the Hamiltonian operator corresponding to the coordinates of the two electrons and the two nuclei for the confined H_2 molecule, as follows

$$\widehat{H} = -\frac{1}{2}\nabla_1^2 - \frac{1}{2}\nabla_2^2 + -\frac{1}{\boldsymbol{r}_{1a}} - \frac{1}{\boldsymbol{r}_{1b}} - \frac{1}{\boldsymbol{r}_{2a}} - \frac{1}{\boldsymbol{r}_{2b}} + \frac{1}{\boldsymbol{r}_{12}} + \frac{1}{R} + V_c \tag{4.7}$$

In this thesis we have considered the case of prolate spheroidal confining box so, we used prolate spheroidal coordinates. It is well known that such a coordinate system consists of families of mutually orthogonal confocal ellipsoids (λ) and hyperboloids (μ) of revolution. The prolate spheroidal coordinates are defined as [46, 47]

$$\lambda = \frac{r_1 + r_2}{D}, \qquad \mu = \frac{r_1 - r_2}{D}. \tag{4.8}$$

The ranges of these variables are

$$1 \le \lambda \le \infty, \qquad -1 \le \mu \le 1. \tag{4.9}$$

The different sets of coordinates (λ_1, μ_1) and (λ_2, μ_2) are assigned, respectively, to electrons characterized by the positions (r_1, r_2) and (r_1^*, r_2^*) relative to the foci as shown in Figure-4.2. In these coordinates, the kinetic-energy operator and the potential-energy operator are written as [46, 47]

$$-\frac{1}{2}\nabla_i^2 = -\frac{2}{D^2\left(\lambda_i{}^2-\mu_i{}^2\right)}\left\{\frac{\partial}{\partial\lambda_i}\left(\lambda_i{}^2-1\right)\frac{\partial}{\partial\lambda_i}+\frac{\partial}{\partial\mu_i}\left(1-\mu_i{}^2\right)\frac{\partial}{\partial\mu_i}\right\} \tag{4.10}$$

$$V = -\frac{4}{D}\left(\frac{\lambda_1}{\lambda_1^2-\mu_1^2}+\frac{\lambda_2}{\lambda_2^2-\mu_2^2}-\frac{1}{2\rho}\right)+\frac{1}{R}+V_c, \tag{4.11}$$

respectively, where $\rho = 2r_{12}/D$.

In Figure-4.1 and Figure-4.2 we presented the geometric characteristics of the confined hydrogen molecular ion H_2^+ and the hydrogen molecule H_2, respectively, confined within a prolate spheroidal cavity defined by ξ_0. In the case of the hydrogen molecular ion H_2^+ the nuclear charges ($Z_a = Z_b = 1$) are both located at distance $\frac{R}{2}$ from the origin. Also, the nuclear charges ($Z_a = Z_b = 1$) for the hydrogen molecule H_2 are both located at distance d_a and d_b from the origin, respectively. D is the interfocal separation and R is the internuclear distance, $R = d_a + d_b$. r_a and r_b are the distances from electron to nuclei $a(b)$, respectively. $r_{1a(b)}$ and $r_{2a(b)}$ are the distances from electrons 1 and 2 to nuclei $a(b)$, respectively, and $r_{1(2)}$, $r^*_{1(2)}$ are their corresponding distances to the foci. r_{12} is the electron–electron distance.

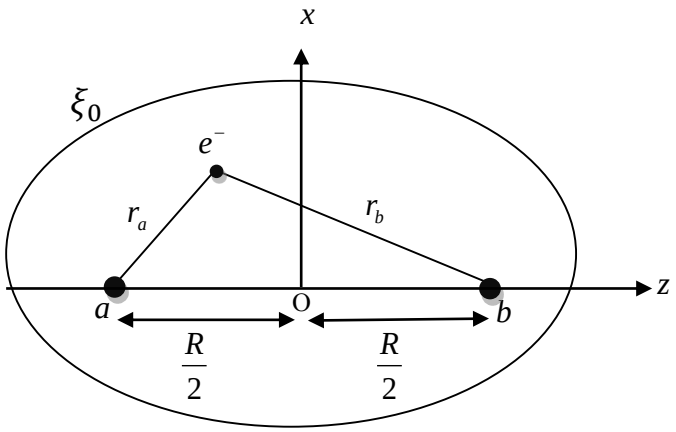

Figure-4.1 Hydrogen molecular ion H_2^+ confined within a prolate spheroidal cavity.

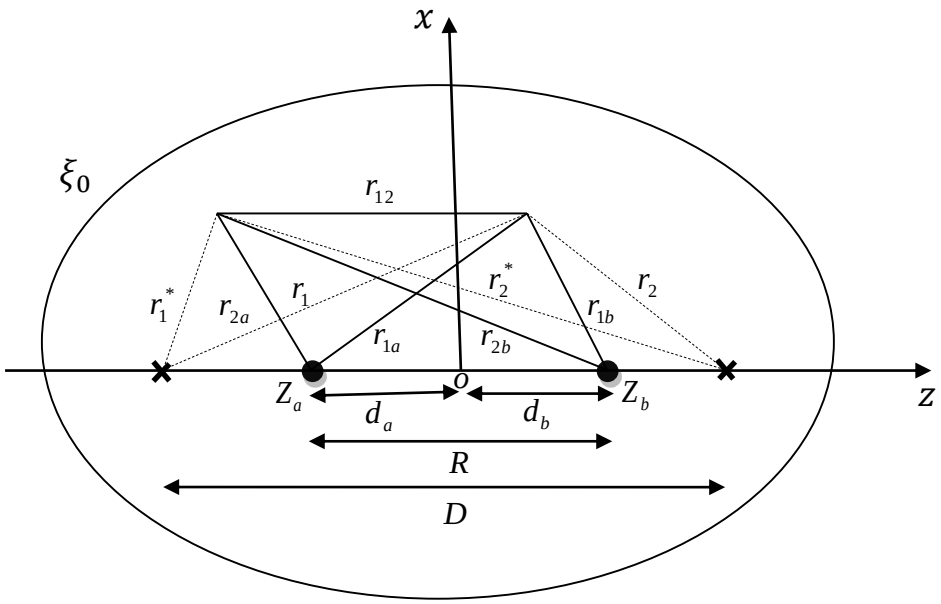

Figure-4.2 Hydrogen molecule H_2 confined within a prolate spheroidal cavity defined by ξ_0.

Our calculations for the ground state of the confined H_2^+ molecular ion and the H_2 molecule are based on using the trial wave functions ψ_1 and ψ_2 which are introduced in chapter 3 and are used to calculate the ground state energy for H_2^+ molecular ion and H_2 molecule. These wave functions are highly compact and have clear physical meaning and satisfy all the boundary conditions. As mentioned in chapter 3 the two functions are given by

$$\psi_1 = \sum_i C_i \, \lambda^{m_i} \, \mu^{n_i} \, exp(-\omega\lambda), \tag{4.12}$$

where C_i are the variational parameters and $\omega = 1.2$ and

$$\psi_2 = \sum_i C_i(1 + p_{12}) \, exp[-\alpha(\lambda_1 + \lambda_2)] \, \lambda_1^{m_i} \, \lambda_2^{n_i} \, \mu_1^{j_i} \, \mu_2^{k_i} \, \rho^{l_i}, \tag{4.13}$$

where p_{12} is an electron exchange operator, C_i are the variational parameters and $\alpha = 3/4$.

For the ground state, the overlap and Hamiltonian integrals of H_2^+ are easily done when the wave functions ψ_1 and ψ_2 are given by Eq. (4.12) and Eq. (4.13), respectively. Here, we discuss the validity of using these compact wave functions to study the Compression effects in H_2^+ ion and H_2 molecule constrained by hard spherical walls. To study the case of H_2^+ ion and H_2 molecule confined by a hard spherical boundary surface the wave functions must vanish at the spherical boundary surface, so a cut-off factor is employed to fulfill this condition and the wave functions become:

$$\psi_1 = \begin{cases} \sum_i C_i \, \lambda^{m_i} \, \mu^{n_i} \, exp(-\omega\lambda) \times \left[\left(1 - \frac{\lambda - 1}{\xi_0 - 1}\right) \; exp\left(\frac{\lambda - 1}{\xi_0 - 1}\right)\right] & \text{for } \lambda < \xi_0 \\ 0 & \text{for } \lambda \geq \xi_0 \end{cases}. \qquad (4.14)$$

and

$$\psi_2 = \begin{cases} \sum_i C_i (1 + p_{12}) \, exp[-\alpha(\lambda_1 + \lambda_2)] \; \lambda_1^{m_i} \, \lambda_2^{n_i} \, \mu_1^{j_i} \, \mu_2^{k_i} \, \rho^{l_i} \, [(1 - \gamma \, \lambda_i/\xi_0)] & \text{for } \lambda < \xi_0 \\ 0 & \text{for } \lambda \geq \xi_0 \end{cases} \quad (4.15)$$

In Eq. (4.14) the last factor in parenthesis represents the cut-off factor $\left[\left(1 - \frac{\lambda - 1}{\xi_0 - 1}\right) \; exp\left(\frac{\lambda - 1}{\xi_0 - 1}\right)\right]$ in terms of the elliptic coordinates and it guarantee that $\psi_1(\lambda = \xi_0, \mu) = 0$ at the boundary. This type of cut-off function was introduced in [67] and it was found that it provides accurate results. Also, the presence of cut-off factor $[(1 - \gamma \, \xi_i/\xi_0)]$ in Eq. (4.15) in parenthesis represents the cut-off factor in terms of the elliptic coordinates and depends on the variational parameter γ is to guarantee that $\psi_2(\lambda = \xi_0, \mu) = 0$ at the boundary. This factor has been successfully used in previous variational studies of atoms confined by padded spherical walls [68] and becomes the usual cut-off term for an infinitely hard wall when $\gamma = 1$,

as discussed in [46]. This type of cut-off function was found to provide accurate results.

4.3 Discussion of the Results of Chapter 4

The Variational Monte Carlo method has been employed for the ground state of the confined molecular ion H_2^+ and the confined molecule H_2. The hydrogen molecular ion H_2^+ and the hydrogen molecule H_2 have the charge parameters $Z_a = Z_b = 1$. All energies are obtained in atomic units i.e. $(\hbar = e = m_e = 1)$ with set of 4×10^7 Monte Carlo integration points in order to make the statistical error as low as possible. This section presents the results obtained with the wave functions which were introduced in the previous section (to calculate the ground state energies of the hydrogen molecular ion H_2^+ and H_2 molecule) and also proposed in chapter 3.

Excellent quantitative agreement is obtained compared to the corresponding exact values. These results validate the accuracy of the wave functions to calculate the ground-state energy $(1s\sigma_g)$ of H_2^+ and H_2 molecule inside a hard prolate spheroidal box under compression. Since molecules when squeezed into a tiny space, they present different electronic and structural behavior in contrast to their free condition; then, knowledge of the way these changes take place as a function of cavity size, shape and composition is of paramount importance.

In the case of H_2^+ we have studied the case in which the nuclei are clamped at the foci and the interfocal distance $D = R = 2$ a.u., and also studied other approximate calculations. The potential barrier parameter V_c can take values between zero and infinity representing walls with increasing confining strength. In Table-4.1 we displayed the results obtained for the

ground-state of the confined H_2^+ molecular ion together with the corresponding results which are available in the literature and the most recent results. The obtained energies were calculated for wide range of ξ_0. The small values of ξ_0 describe the case of strong confinement where the large values represent the weak compression. It is clear that our results are of good agreement in comparison with previous data. The agreement with other data is found to be good even for relatively large values of the eccentricity $1/\xi_0$. We report the results obtained in Ref [66] here as the electronic energy where the total electronic energy of the molecular ion H_2^+ is defined as the total energy E_T minus the repulsive energy between the nuclei, $E_{ele} = E_T - \frac{Z_a Z_b}{R}$.

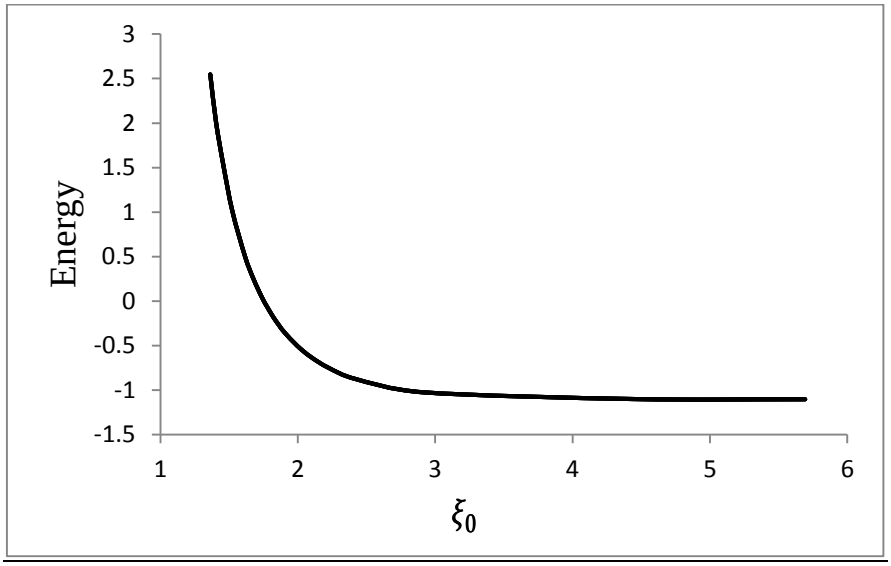

Figure-4.3 The ground-state energy of H_2^+ versus ξ_0.

Figure-4.3 shows the variation of the ground-state energy with respect to ξ_0. It is clear from Figure-4.3 that the energies increase when ξ_0 decreases for strong compression at $\xi_0 < 2.9162$ where for large values of $\xi_0 \geq$

2.9162, the compression effect becomes not noticeable and the energy is nearly stable and approaches to the corresponding exact value, i.e. when ξ_0 increases that leads to less energy to reach even the free state of H_2^+. Also, Figure-4.3 insures the fact that the energy of the low-lying states in a confined quantum charged system is determined by a competition of confinement kinetic energy and Coulomb interaction energy. As the molecules are compressed, they become constrained in a diminishing spherical box so that according to the quantum mechanical uncertainty principle, the electrons increase their momentum and thereby leading to a net gathering of kinetic energy. In other meaning the smaller the confined potential spheroidal cavity ξ_0 is, the higher the confinement kinetic energy is. When the increase in the confinement kinetic energy becomes predominant and cannot be compensated by the increase of the Coulomb attractive energy, the energies of the confined H_2^+ increase.

On the other hand, Table-4.2 displays the results for the energy evolution of the $(1s\sigma_g)$ state of the confined H_2^+ molecular ion within a prolate spheroidal cavity with fixed major axis $C = R\xi_0 = 5$ a.u. and different values for the internuclear distance R, compared to the corresponding exact calculations by Mateos *et al.* [69] and other approximate calculations. The agreement with other data is found to be good.

Table-4.1 The electronic energy of the ground state of H_2^+ obtained using the wave function of Eq. (4.14) with a fixed internuclear distance $R = R_0 = 2\,\text{a.u}$ and different sizes and ξ_0 as compared with the exact and other approximate calculations. In parentheses, we show the statistical error in the last figure.

ξ_0	$E_{\text{this work}}$	E^a	E^b	E^c	E^d_{exact}
5.6924	-1.1024920(1)	-1.1022	-1.1022	-	-1.1025
4.4468	-1.099999(1)	-	-	-1.099991	-1.1
2.9162	-1.024930(5)	-	-1.0237	-	-1.025
2.4196	-0.8749254(6)	-	-0.8746	-0.875027	-0.875
2.2237	-0.7497891(4)	-0.7499	-0.75	-	-0.75
2.0917	-0.6249598(6)	-	-	-0.624975	-0.625
1.9934	-0.499707(8)	-0.4999	-0.4999915	-	-0.5
1.9002	-0.347878(2)	-	-	-0.3467505	-0.35
1.8638	-0.274803(2)	-	-	-	-0.275
1.8186	-0.174838(2)	-	-	-0.1750125	-0.175
1.7788	-0.072020(3)	-	-	-	-0.075
1.7606	-0.024874(4)	-	-	-	-0.025
1.7434	0.02568442(2)	0.0258	-	-	0.025
1.7270	0.07647589(4)	-	-	-	0.075
1.7115	0.1275443(3)	-	-	-	0.125
1.6690	0.2756515(1)	-	-	-	0.275

Table-4.1 Continued

ξ_0	$E_{\text{this work}}$	E^a	E^b	E^c	E^d_{exact}
1.6150	0.5012(3)	0.5025	0.5072	-	0.5
1.5229	1.0095(4)	-	-	-	1.0
1.4555	1.541445(1)	-	-	-	1.5
1.4035	2.015272(1)	-	-	-	2.0
1.3621	2.544751(1)	2.5214	-	-	2.5

[a] Ref [65] [b] Ref [66] [c] Ref [71] [d] Ref [70]

Finally, our results were extended to include the HeH^{++} molecular ion which has the charge parameters $Z_a = 2$, $Z_b = 1$. Table-4.3 shows the results for the energy evolution of the $(1s\sigma_g)$ state of the confined HeH^{++} molecular ion confined by a hard prolate spheroid characterized by an internuclear distance $R = 2$ a. u. with different sizes and eccentricities. Also, the corresponding exact calculations by Ley-Koo *et al*. [70] and accurate variational calculations from Ref [65] are presented for comparison. The comparison insures that our results are of good accuracy. It is clear that the obtained numerical results are in good agreement with the exact and other approximate calculations.

Table-4.2 Total energy behavior of the ground state energy of H_2^+ enclosed by a prolate spheroidal cavity with major axis $C = R\xi_0 = 5$ a.u. and varying internuclear distances. In parentheses, we show the statistical error in the last figure.

R	$E_{\text{this work}}$	E^a	E^b_{exact}
1.1	-0.4190592(5)	-0.4287	-0.429173
1.4	-0.4705254(1)	-0.4716	-0.471751
1.5	-0.4710616(2)	-0.4703	-0.471784
1.6	-0.4657539(1)	-0.4657	-0.466979
1.9	-0.4301752(3)	-0.4294	-0.430244
2.2	-0.3669057(2)	-0.3665	-0.366949
2.5	-0.2790038(8)	-0.2789	-0.279130
2.8	-0.1631775(1)	-0.1634	-0.163430

[a] Ref [65] [b] Ref [69]

Table-4.3 The electronic energy of the $(1s\sigma_g)$ of HeH^{++} with nuclear positions located at the foci of a confining prolate spheroidal cavity of internuclear distance $R = 2$ a.u. with different sizes and ξ_0. In parentheses, we show the statistical error in the last figure.

ξ_0	$E_{\text{this work}}$	E^a	E^b_{exact}
1.7025	-1.49919(6)	-	-1.5
1.6580	-1.324248(6)	-	-1.325
1.6410	-1.248159(1)	-1.2498	-1.25
1.5914	-0.9999956(1)	-	-1.0
1.5499	-0.749947(3)	-0.7498	-0.75
1.5424	-0.6991266(3)	-	-0.7
1.5351	-0.6499709(4)	-	-0.65
1.5211	-0.5487804(5)	-0.5498	-0.55
1.5144	-0.4995019(4)	-	-0.5
1.4833	-0.2492223(8)	-	-0.25
1.4558	0.000497736(7)	-	0.0
1.4313	0.2515458(8)	0.2519	0.25
1.4091	0.5058985(1)	-	0.5
1.3705	1.056358(5)	1.0066	1.0
1.3379	1.502523(5)	-	1.5

[a] Ref [65] [b] Ref [70]

Also, we have studied the case of hydrogen molecule confined by a hard prolate spheroidal cavity in two cases, when the nuclear positions are clamped at the foci (on-focus) and the case of off-focus nuclei in which the two nuclei are uncoupled from the foci (not clamped at the foci).

Firstly, we study the case in which the nuclei are clamped at the foci $d_a = d_b = D/2$, once a major axis ($D\xi_0, D = R = d_a + d_b$) is fixed, variation of the internuclear distance $(R = D)$ necessarily implies a change in eccentricity $(1/\xi_0)$, which corresponds to a different cage geometry. In Table-4.4 we displayed the results obtained for the ground state of the confined H_2 molecule within a prolate spheroidal cavity with various major axis $C = R\xi_0$ and different values for the internuclear distance R together with the corresponding accurate variational calculations by Lesar *et al*. [72, 73], Cruz *et al*. [46] and exact QMC calculations by Pang [74]. The agreement with other data is found to be good even for relatively large values of the eccentricity, $(1/\xi_0)$.

Table-4.4 Ground-state energies obtained in this thesis for the H_2 molecule confined within hard prolate spheroidal boxes with nuclear positions clamped at the foci for selected values of the major axis ($R\xi_0$) as compared with the corresponding accurate calculations. In parentheses, we show the statistical error in the last figure.

$R\xi_0$	R	$E_{\text{this work}}$	E^a	E^b	E^c
∞	1.388	-1.133296(1)	−1.1332	-	-
	1.4010	-1.173397(1)	-	-	-1.1746
12	1.386	-1.132001	−1.1322	-	-
	1.403	-1.156829	-	−1.1685	-
10	1.372	-1.128147(4)	−1.1292	-	-
	1.395	-1.162297(2)	-	−1.1638	-
8	1.321	-1.11102(3)	−1.1102	-	-
	1.3503	-1.1500(3)	-	-	−1.1533
6	1.1771	-1.0515(2)	-	-	−1.0523
	1.208	-1.040882(1)	-	−1.0441	-
4	0.885	-0.431810(4)	−0.4321	-	-
	0.893	-0.4744763(6)	-	−0.4749	-
	0.8949	-.4786076(1)	-	-	−0.4790
3	0.683	0.6932845(2)	0.6934	-	-
	0.686	0.647240(1)	-	0.6474	-
2	0.4493	4.595042(5)	-	-	4.5944
	0.454	4.644851(5)	4.6433	-	-

[a] Ref [56]. [b] Ref [75]. [c] Ref [46].

Now, let the two nuclei are allowed to relax out of the focal positions along the major axis. This means that the internuclear distance R and the interfocal distance D have slightly different values from each other. The obtained results for this case are listed in Table-4.5. By comparing the results obtained in relaxation case (Table-4.5) and those of clamped case (Table-4.4) this reflects the effect of the relaxation of the on-focus nuclei. The comparison ensures that the optimum value of the energy can be obtained when the nuclei do not coincide with the foci. Also, the equilibrium internuclear distances increase relative to the on-focus case with corresponding lowering in the energy. The independence of confining box size and shape on the nuclear positions provide us with additional degree of freedom by controlling the shape and size of the confining box while varying the nuclear positions.

Figure-4.4 shows in more detail the evolution of the total energy behavior of the ground state energy as a function of ξ_0 and the internuclear distance R of H_2 molecule enclosed by a prolate spheroidal cavity with major axis $D\xi_0$ for the set of box sizes considered here after allowing for nuclear relaxation in the corresponding on-focus calculations.

Table-4.5 Total energy behavior of the ground state energy of H_2 molecule enclosed by a prolate spheroidal cavity with major axis $D\xi_0$ after allowing for nuclear relaxation in the corresponding on-focus calculations. D is the original equilibrium on-focus bond length. In parentheses, we show the statistical error in the last figure.

$D\xi_0$	D	R	$E_{\text{this work}}$	E^a
12	1.386	1.391	-1.1328(1)	-1.1322
10	1.372	1.376	-1.1230(1)	-1.1292
8	1.321	1.323	-1.1101(7)	-1.1102
6	1.177	1.187	-1.0069(7)	-1.0081
4	0.885	0.913	-0.4337252(1)	-0.4333
3	0.683	0.726	0.6875051(1)	0.6878
2	0.454	0.508	4.622613(7)	4.6142

[a] Ref [46].

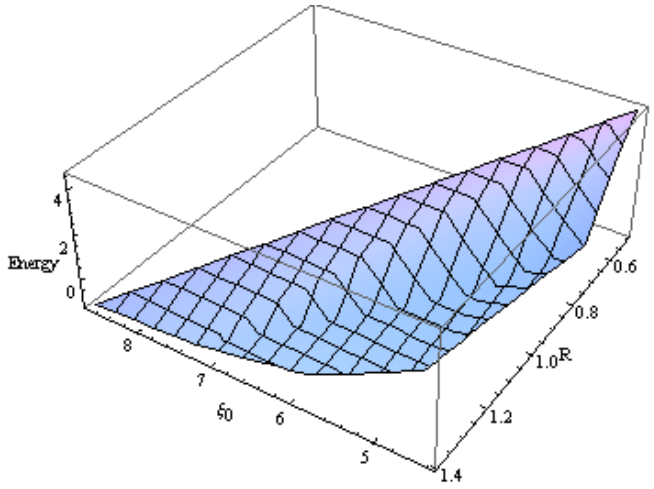

Figure-4.4 Total energy behavior of the ground state energy as a function of ξ_0 and the internuclear distance R of H_2 molecule enclosed by a prolate spheroidal cavity with major axis $D\xi_0$ after allowing for nuclear relaxation in the corresponding on-focus calculations.

On the other hand, we have considered the case of off-focus nuclear positions with fixed eccentricity $e = \frac{1}{\xi_0} = 0.5$. In this case the shape of the cavity will kept fixed where the size is variable. Consider the case in which H_2 molecule is compressed within a prolate spheroidal cavity with variable sizes for different values of major axis $C = D\xi_0 = 2, 3, 4, 6, 12$ and different values for the internuclear distance R. The results describing this case are displayed in Table-4.6. In this technique, all boxes keep the same aspect ratio as the volume changes. In this table we compare our results with the first results obtained previously for this case by Cruz *et al*. [46]. It is clear that our results exhibit a good accuracy compared to previous data. The obtained results are presenting for the case of off-focus nuclear relaxation for a fixed confining geometry leading to new energies as compared to the corresponding on-focus calculation.

Table-4.6 Total energy behavior of the ground state energy of H_2 molecule enclosed by a prolate spheroidal cavity with varying major axis $C = D\xi_0 = 2, 3, 4, 6, 12$ and fixed eccentricity $e = \frac{1}{\xi_0} = 0.5$. In parentheses, we show the statistical error in the last figure.

$D\xi_0$	R	$E_{\text{this work}}$	E^a
12	1.381	-1.126886(4)	-1.1268
6	1.153	-0.9311808(2)	-0.9392
4	0.880	-0.1938857(1)	-0.1938
3	0.704	1.212303(2)	1.2141
2	0.490	5.989710(1)	5.9899

[a] Ref [46].

Figure-4.5 represents the variation of the energy versus the internuclear distance *R* for the free and confined H_2 molecule. It is clear that the energy increases in both free and confined cases under decrease of the internuclear distance *R*.

Now, we will introduce a simple chemical analysis concerning the catalytic role of enzyme. Enzymes are macromolecular biological catalysts which play a central role in life due to their catalytic properties. The molecules at the beginning of the process are called substrates and the enzyme converts these into different molecules, called products. The active site is always a non-rigid polar cavity, or crevice, where the substrate will be rearranged in products. There are two cases for converting from the confined state to the free state. Considering a confined molecule with the energy given in point A. In the first case, let us assume a sudden release of the

constraint, this will relax the bonding electron into the free state with similar internuclear distance *R*. In this hypothesis, the vertical transition of the electrons from A → *B* (or from confined to unconfined state) leads to change the free molecule state and leaves it in a vibrational excited state. In the second case, if the switch-off of the constraint is slower, the relaxation pathway becomes A → *C*. In this relaxation pathway the nuclei have time to move and so they gain kinetic energy. Hence, the chemical bond is left in a vibrational excited state. In case of strong compression, then molecular bond scission might be obtained however, we can stat that in all cases the molecular bond of the free molecule on its electronic ground state is left, at least, in a vibrational excited state. As a result, one can consider the behavior of the vibrational excitation (or bond breaking) to be like the effect of increasing the temperature of the substrate which leads to easier a subsequent atomic rearrangement to give the products. This is a fundamental property, essential for the catalytic role of enzyme.

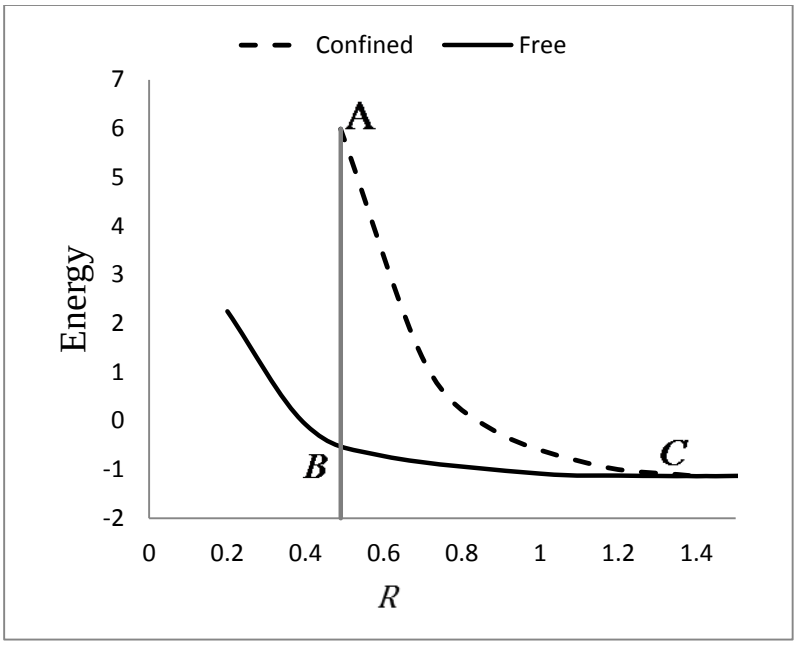

Figure-4.5 Change of the ground state energy of a confined H_2 molecule when the confinement is removed. Two different situations are illustrated.

4.4 Conclusion

In frame of the Variational Monte Carlo method we calculated the H_2^+ molecular ion and H_2 molecule confined within hard prolate spheroidal boxes. We have calculated the energies for both confined H_2^+ molecular ion and H_2 molecule. In the case of H_2^+ molecular ion, we considered the case of small values of ξ_0 which describe the strong compression as well as the case of large values of ξ_0. Our results were extended also to include the HeH^{++} molecular ion. The energy was plotted as a function of ξ_0 to show graphically the effect of compression on the total energy. The graphs indicate that the values of the energy are affected significantly at small values of ξ_0, where at large values the energy tends to be constant and approaches to its uncompressed value. In the case of H_2 molecule, ground-state energies obtained for the H_2 molecule confined within hard prolate

spheroidal boxes with nuclear positions clamped at the foci for selected values of the major axis ($R\xi_0$) as compared with corresponding accurate calculations. It was shown also here that, when the nuclear positions are allowed to relax out of the foci for a fixed cage size and shape, different energies are obtained. Also, the case of off-focus nuclei in which the two nuclei are uncoupled from the foci is studied. In all cases our results exhibit good accuracy comparing with previous values obtained by using different methods and different forms of trial wave functions. Finally, we conclude that the applications of VMC method can be extended successfully to cover the case of compressed molecules.

Chapter 5

Ground States of the Hydrogen Molecule and Its Molecular Ion in the Presence of Magnetic Field Using the Variational Monte Carlo Method

5.1 Introduction

The influence of a magnetic field on the properties of molecules is of great interest. The simplest molecules (the hydrogen molecular ion H_2^+ and the hydrogen molecule H_2) allow for the studying of their properties in strong magnetic fields with high accuracy. These molecule–field systems have an essential importance not only in atomic and molecular physics but also in astrophysics, semiconductor physics, solid state and plasma physics [76].

The behaviour of the H_2^+ molecular ion and the hydrogen molecule H_2 under strong magnetic field conditions has been studied by many authors. Most of them deal with the hydrogen molecular ion H_2^+ and little is known about the hydrogen molecule H_2. Research on the behaviour of molecules in strong fields is more complicated than that of atoms because of the multi-center characteristics of the molecules.

The total energies and the equilibrium internuclear separations of H_2^+ molecular ion in states σ_g, π_u, δ_g, ϕ_u, γ_g, η_u in strong magnetic fields have been calculated using the adiabatic approximation and adiabatic variational approximation with an effective potential by Yong *et. al* [77].

Using the two-dimensional pseudospectral method the ground and low-lying states of the H_2^+ molecular ion in a strong magnetic field are calculated in Ref [78]. The hydrogen molecular ion H_2^+ aligned with a magnetic field has been studied with the Lagrange-mesh method which allows obtaining highly accurate results under various field strengths and

for various quantum numbers [79]. Turbiner *et al.* [80] studied the qualitative and quantitative consideration of the one-electron molecular systems such as H_2^+, H_3^{2+} and H_4^{3+} in the presence of a magnetic field.

Using an accurate one center method with a technique that combining the spheroidal coordinate and B-spline, Zhang et al. [81-83] have calculated the equilibrium distances and the hydrogen molecular ion H_2^+ in both ground and low-lying states in the presence of a magnetic field. Also, the hydrogen molecular ion in a strong magnetic field has been studied for arbitrary orientations of the molecular axis in the non-aligned case by using the Lagrange-mesh method to obtain highly accurate results under these assumptions at various field strengths [84].

Using the time-dependent density functional theory the variations in electron density and bonding have been investigated for the lowest $1\sigma_g$ state of the hydrogen molecule under strong magnetic fields [85]. Song *et al.* [86] calculated the electronic structure and properties of the hydrogen molecule H_2 for the lowest $1\sigma_g$ and $1\sigma_u$ state in parallel magnetic fields using a full configuration-interaction (CI) method which is based on the Hylleraas-Gaussian basis set.

The aim of this chapter is to study the total energies, the dissociation energies and the binding energies for the hydrogen molecular ion H_2^+ and the hydrogen molecule H_2 in the presence of external magnetic field in framework of the variational Monte Carlo method.

5.2 The Hamiltonian of the System

In the present thesis, we assume that the nuclear mass is infinite so that the calculations will be one in frame of the Born–Oppenheimer approximation and the magnetic field is oriented along the z-axis. The Schrödinger equation can be written as follows

$$\hat{H}\psi(\boldsymbol{r_i}, R) = E\psi(\boldsymbol{r_i}, R) \tag{5.1}$$

where $\boldsymbol{r_i} = (x_i, y_i, z_i)$ are the coordinates of each electron with respect to the center of mass of the nuclei, $i = 1, 2$ and R is the internuclear distance. The non-relativistic Hamiltonian $\hat{H}$ for the hydrogen molecular system in a magnetic field can be written as

$$\hat{H} = -\frac{1}{2}\sum_{i=1}^{n} \nabla_i^2 - \sum_{i=1}^{n}\left(\frac{Z_a}{r_{ia}} + \frac{Z_b}{r_{ib}}\right) + \frac{Z_a\, Z_b}{r_{12}} + \frac{Z_a\, Z_b}{R} + H_M \tag{5.2}$$

In the above equation, $r_{ia(b)} = \left|\boldsymbol{r}_{ia(b)}\right|$ denotes the distance from electron 'i' ($i = 1, 2$) to nucleus 'a' ('b'), the charge parameters $Z_a = Z_b = 1$, r_{12} is the interelectronic distance and H_M represents the magnetic part. The magnetic Hamiltonian term for a magnetic field of intensity B directed towards the positive $Z - axis$ takes the form

$$H_M = \begin{cases} \frac{\gamma}{2} L_z + \frac{\gamma^2}{8}\,\rho^2, & \text{for } H_2^+ \\ \frac{\gamma^2}{2}\rho^2 + \gamma(L_z + 2S_Z) & \text{for } H_2 \end{cases} \tag{5.3}$$

where, $\gamma = \frac{B}{B_0}$ ($B_0 \approx 2.35 \times 10^5$ T) is the magnetic field strength, L_z is the z-component of the total angular momentum, S_z is the z-component of the total spin and $\rho^2 = \sum_{i=1}^{n}(x_i^2 + y_i^2)$. The index n runs over the numbers of the electrons. Then, for the hydrogen molecule, H_2, $n = 2$. For the hydrogen molecular ion, H_2^+, $n = 1$ and the term $\frac{Z_a\, Z_b}{r_{12}}$ is omitted.

Hence, the non-relativistic Hamiltonian $\hat{H}$ for the hydrogen molecular ion H_2^+ in a magnetic field can be written as [79, 83]:

$$H = -\frac{1}{2}\nabla^2 - \frac{1}{r_a} - \frac{1}{r_b} + \frac{1}{R} + \left[\frac{\gamma}{2} L_z + \frac{\gamma^2}{8}\,\rho^2\right], \tag{5.4}$$

where $r_a = |\boldsymbol{r}_a|$ and $r_b = |\boldsymbol{r}_b|$ in which $\boldsymbol{r}_a$ and $\boldsymbol{r}_b$ denote the relative radius vectors of the electron with respect to the two nuclei a and b and $\rho^2 = (x^2 + y^2)$.

Similarly, the molecular electronic Hamiltonian for the hydrogen molecule H_2 under a magnetic field may be conveniently written (in atomic units) as follows [87]

$$H = -\frac{1}{2}\nabla_1^2 - \frac{1}{2}\nabla_2^2 - \frac{1}{r_{1a}} - \frac{1}{r_{1b}} - \frac{1}{r_{2a}} - \frac{1}{r_{2b}} + \frac{1}{r_{12}} + \frac{1}{R} + \left[\frac{\gamma^2}{2}\rho^2 + \gamma(L_z + 2S_Z)\right] \quad (5.5)$$

In the above equation, $\rho^2 = (x_1^2 + y_1^2) + (x_2^2 + y_2^2)$.

Equation (5.2) is best treated in the system of prolate spheroidal coordinates (λ, μ) where λ and μ are defined by

$$\lambda = \frac{r_{ia} + r_{ib}}{R}, \qquad \mu = \frac{r_{ia} - r_{ib}}{R} \quad (5.6)$$

In these coordinates, the kinetic-energy operator is written as

$$-\frac{1}{2}\nabla_i^2 = -\frac{2}{R^2\left(\lambda_i^2 - \mu_i^2\right)}\left\{\frac{\partial}{\partial\lambda_i}\left(\lambda_i^2 - 1\right)\frac{\partial}{\partial\lambda_i} + \frac{\partial}{\partial\mu_i}\left(1 - \mu_i^2\right)\frac{\partial}{\partial\mu_i}\right\} \quad (5.7)$$

Our calculations for the ground state of H_2^+ molecular ion and H_2 molecule in the presence of external magnetic field are based on using the trial wave functions ψ_1 and ψ_2 which are introduced in Chapter 3 and they are given by equation (3.13) and equation (3.14).

Figure-5.1 and Figure-5.2 represent illustrations for the hydrogen molecular ion and the hydrogen molecule.

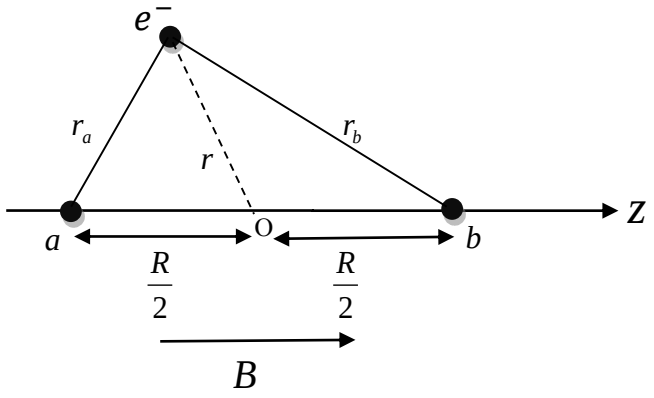

Figure-5.1 Geometrical setting for the hydrogen molecular ion H_2^+ placed in a magnetic field directed along the z-axis. The protons are situated at a distance R from each other.

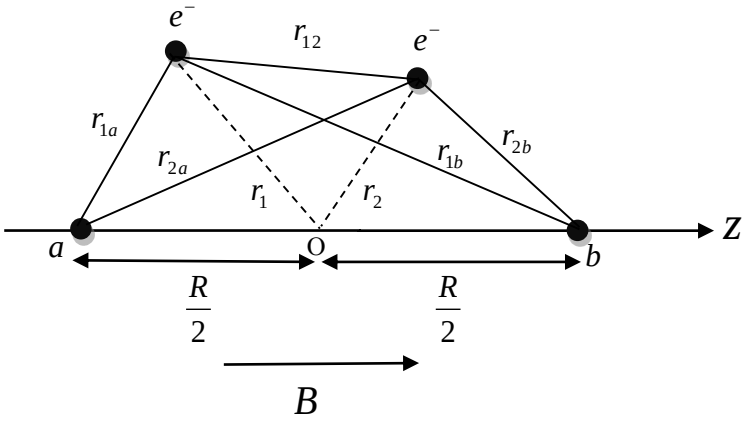

Figure-5.2 Geometrical setting for the hydrogen molecule H_2 placed in a magnetic field directed along the z-axis. The protons are situated at a distance R from each other.

5.3 Discussion of the Results of Chapter 5

The variational Monte Carlo method has been employed to calculate the ground state of the hydrogen molecular ion H_2^+ and the hydrogen molecule H_2 in the magnetic field regime between 0 a.u. and 10 a.u.. All energies are obtained in atomic units i.e. ($\hbar = e = m_e = 1$) with set of 4×10^7 Monte Carlo integration points in order to make the statistical error as low as possible. The magnetic field was taken in the parallel configuration, i.e. the angle between the molecular axis and the magnetic field direction is zero, $\theta = 0^o$ as shown in Figure-5.1 and Figure-5.2. In the absence of magnetic field, our results for the total energy of the hydrogen molecular ion H_2^+ in the lowest state ($1s\sigma_g$) equals -0.6023424 at the equilibrium distance of $R = 1.9972$ a.u, where for hydrogen molecule H_2 the total energy equals -1.173427 at $R = 1.40$ a.u.

In this thesis we have calculated the total energies, the binding energies and the dissociation energies of the ($1s\sigma_g$) state as functions of the magnetic field over various field-strength regimes (0 - 10 a.u.). The total energy E_T of the hydrogen molecular ion H_2^+ and the hydrogen molecule

H_2 is defined as the total electronic energy plus the repulsive energy between the nuclei, $E_T = E_{ele} + \frac{Z_a Z_b}{R}$. The least energy required to produce a free electron and two nuclei, all infinitely far from each other in the presence of the field has been defined as the binding energy for the hydrogen molecular ion H_2^+: $E_b = \frac{\gamma}{2} - E_T$ by Larsen in [88]. For the hydrogen molecular ion H_2^+, the dissociation energy is defined as the least energy required to dissociate the molecule into one nucleus and one hydrogen atom in a magnetic field, $E_d = E_H - E_T$ where E_H is the total energy of the hydrogen atom in a magnetic field, i.e. the product of the process $H_2^+ \rightarrow H + P^+$ [88].

In the case of the hydrogen molecule H_2, the product is $H_2 \rightarrow H(1s) + H(1s)$ which means that the energy in the dissociation limit corresponds to the energy of two hydrogen atoms in the lowest electronic state with positive z parity i.e., the quantity $E_d = E_T - \lim_{R\rightarrow\infty} E_T$. The binding energy is equal to the ionization energy and is always greater than the dissociation energy. The presence of free electron in the orbitals of molecules will cause an induced magnetic field, to be produced, and also due to the spin motion of this free electron. We observe this in the hydrogen molecular ion H_2^+ where, the presence of one electron in the $1s$ orbital will cause a weak induced magnetic field by the spin motion of this electron either clockwise or counterclockwise. Also, we showed that there is no induced magnetic field in the hydrogen molecule H_2 as two electrons are paired in $1s$ orbital. The strength of the magnetic field is directly proportional to the odd number of free electron present in the orbitals.

The present calculations in the presence of a magnetic field are based on using the trial wave functions ψ_1 and ψ_2 which are introduced in Chapter 3 and are given by Eq. (3.13) and Eq. (3.14), respectively. For hydrogen molecular ion, the total energies are obtained by solving the Schrödinger

equation given by Eq. (5.1) by using ψ_1. Table-5.1 represents the obtained results for H_2^+. In our calculations the values of E_H are taken from Ref [78]. In a similar way, the total energies, and the dissociation energies as functions of the magnetic field over various field-strength regimes are presented in Table-5.2 for the ground $1s\sigma_g$ state of the hydrogen molecule H_2.

From Table-5.1 and Table-5.2, we can observe that the binding energy, the dissociation energy and the total energy increase with the increase in the magnetic field strength. This is due to that the increase in the field strength leads to increases in the movement of the electron and the electronic spatial distribution will be strongly confined in a smaller space. The probability of finding the electron in the region confined by the two nuclei becomes larger under increase of the field strength. So, the changes in the electronic properties of the ground state should be attributed to the increased electron density in the region between the nuclei centered at $z = 0$.

An interesting and general phenomenon for molecules is the decrease of the internuclear bond-length as the field strength increases. The decrease in the equilibrium internuclear distance originates from the simultaneous decrease of the electron clouds perpendicular and parallel to the magnetic field. This means that this state is the most tightly bound state for all magnetic field strengths because the electrons are in this state much closer to the nuclei than in the free-state. This increases the binding due to the attractive nuclear potential energy. Because the dissociation energy may be used to measure the stability of a molecular system in a magnetic fields, it is useful to explore the behaviour of this quantity with increasing field strength. There is an increase in the binding energy of molecular systems as the magnetic field strength gets larger. The increase in the binding

energy comes from the result of strong localization of the electrons around the nuclei. The electron-electron Coulomb repulsion is taken into account.

It is interesting to compare our results with the previous results which used different wave functions and different methods such as [78, 79, 89] for the ground state $1s\sigma_g$ of the H_2^+ molecular ion and [86, 90, 91] for the ground state $1s\sigma_g$ of the hydrogen molecule H_2. It is clear that our results are in good agreement with the pervious data.

Figure-5.3 and Figure-5.4 show the variation of the ground state energy of the H_2^+ molecular ion and the hydrogen molecule H_2 in the presence of a magnetic field from $\gamma = 0.0$ to $\gamma = 10.0$, respectively, versus the internuclear distance R. These show that when the magnetic field strength increases the ground state energy increases as seen from the change in the values of the ground state energy from $\gamma = 0.0$ to $\gamma = 10.0$. We can observe in both cases that at $\gamma = 10.0$ the value of the total energy is the highest energy. At $\gamma = 0.0$ the total energy of the hydrogen molecular ion H_2^+ is larger than the hydrogen molecule because of the induced magnetic field.

Table-5.1 Total energy E_T, binding energy E_b and dissociation energy E_d of the ground state $1s\sigma_g$ of the H_2^+ molecular ion in a parallel magnetic field from $\gamma = 0.0$ to $\gamma = 10.0$. Note in Table-5.1 that the present definition for E_T is equivalent to the definition of E_e in Wille's work [92]. In parentheses, we show the statistical error in the last figure.

γ	R_{eq}	References	E_T	E_b	E_d
0.0	1.9971934	This work	-0.602501700(4)	0.602501700	0.102501700
		[79]	−0.6026346191066	-	-
	1.997193	This work	-0.602501700(4)	0.602501700	0.102501700
		[78]	−0.602634619	0.602634619	0.102634619
	1.9971	This work	-0.602390800(2)	0.602390800	0.102390800
		[89]	−0.602625	0.602625	-
0.002	1.99719	This work	-0.602508600(1)	0.603508600	0.102509600
		[93]	−0.60263398	0.60363398	0.10263498
0.008	1.997162	This work	-0.602477700(2)	0.606477700	0.102493699
		[78]	−0.602624361	0.606624361	0.102640360
	1.99716	This work	-0.602610500(1)	0.606610500	0.102626499
		[93]	−0.60262436	0.60662436	0.10264036
0.02	1.996991	This work	-0.602479700(2)	0.612479700	0.102579656
		[78]	−0.602570515	0.612570515	0.102670471
0.1	1.992212	This work	-0.600764400(0)	0.6507644	0.10323792
		[78]	−0.601038207	0.651038207	0.103511727
	1.9922107	This work	-0.600734200(0)	0.6507342	0.10320772
		[79]	−0.6010382074075	-	-
	1.99221	This work	-0.600685200(0)	0.6506852	0.10315872
		[93]	−0.60103820	0.65103820	0.10351172

Table-5.1 Continued

γ	R_{eq}	References	E_T	E_b	E_d
0.425434	1.924	This work	-0.575015700(2)	0.7877327	0.114587838
		[92]	−0.575359	0.788125	-
	1.9234	This work	-0.574840800(1)	0.787565	0.114412938
		[78]	−0.575370830	0.788087830	0.114942968
	1.9	This work	-0.574771100(3)	0.7874881	0.114343238
		[94]	−0.575075	0.763412	0.114685
1.0	2.0	This work	-0.470237300(5)	0.9702373	0.139068403
		[79]	−0.47054001262014	-	-
		[82]	−0.4705400126203	-	-
	1.752084	This work	-0.468984500(5)	0.9689845	0.137815603
		[82]	−0.474988245275	-	-
		[79]	−0.474988245275	-	-
	1.7520838	This work	-0.468984500(5)	0.9689845	0.137815603
		[79]	−0.474988245275	-	-
	1.7521	This work	-0.468523800(8)	0.9685238	0.1373549033
		[78]	−0.474988245	0.974988245	0.143819348
	1.752	This work	-0.468317700(7)	0.9683177	0.137148803
		[88]	−0.4749	0.9749	-
2.12717	1.5025	This work	-0.17393060(3)	1.2375156	0.1952071163
		[78]	−0.174910873	1.238495873	0.153634357
	1.448	This work	-0.1520147(1)	1.2155997	0.1732912163
		[95]	−0.15225	1.215835	0.2570

Table-5.1 Continued

γ	R_{eq}	References	E_T	E_b	E_d
3.0	1.376	This work	0.10122530(7)	1.3987747	0.2342417107
		[89]	0.10485	1.39515	-
	1.3754	This work	0.10123410(7)	1.3987659	0.2342329107
		[78]	0.104455347	1.39554465	0.231011664
4.25434	1.2465	This work	0.5304074(1)	1.5967626	0.2892954573
		[78]	0.544794264	1.582375737	0.274908594
	1.2464	This work	0.5305169(1)	1.5966531	0.2891859573
		[89]	0.544895	1.5823	-
	1.246	This work	0.530954(1)	1.596216	0.2887488573
		[92]	0.545154	1.582016	-
10.0	0.957	This work	2.8221030(5)	2.177897	0.430107
		[78]	2.825014	2.174986	0.427196
	0.950	This work	2.827940(4)	2.17206	0.42427
		[96]	2.8327	2.1673	0.41955
		[92]	2.8250	2.1750	-

Table-5.2 Total energy E_T, and dissociation energy E_d of the ground state $1s\sigma_g$ of the hydrogen molecule H_2 in a parallel magnetic field from $\gamma = 0.0$ to $\gamma = 10.0$. In parentheses, we show the statistical error in the last figure.

γ	R_{eq}	References	E_T	E_d
0.0	1.40	This work	-1.173427(1)	0.173429
		[90]	−1.173436	0.173438
		[86]	−1.1744477	0.1744478
0.001	1.40	This work	-1.17342(1)	0.173422
		[90]	−1.173436	0.173438
0.005	1.40	This work	-1.173285(1)	0.173301
		[90]	−1.173424	0.173440
0.01	1.40	This work	-1.172867(1)	0.1729171
		[90]	−1.173396	0.173450
		[86]	−1.1744096	0.1744597
0.05	1.40	This work	-1.171858(1)	0.1731047
		[90]	−1.172407	0.173658
		[86]	−1.173497	0.1747437
0.1	1.40	This work	-1.170512(7)	0.1754591
		[86]	−1.1706617	0.1756088
	1.39	This work	-1.166586(5)	0.171542
		[90]	−1.169652	0.174608
0.2	1.39	This work	-1.135232(1)	0.154469
		[90]	−1.158766	0.178001
		[86]	−1.159579	0.178816

Table-5.2 Continued

γ	R_{eq}	References	E_T	E_d
0.4254414	1.349	This work	-1.110247(2)	-
		[90]	−1.110362	
	1.337	This work	-1.079712(1)	-
		[91]	−1.0822	
0.5	1.33	This work	-1.078379(2)	0.183958
		[90]	−1.089082	0.194663
		[86]	−1.089750	0.195329
1.0	1.23	This work	-0.8866(7)	0.224262
		[86]	−0.891184	0.228846
2.0	1.09	This work	-0.3334(2)	0.288972
		[90]	−0.335574	0.291170
		[86]	−0.336236	0.291808
2.127207	1.07	This work	-0.2501(1)	-
		[90]	−0.255591	
4.254414	0.898	This work	1.2322(5)	-
		[90]	1.233808	
	0.859	This work	1.3266(4)	-
		[91]	1.3326	
5.0	0.86	This work	1.8077(5)	0.4459257
		[90]	1.801212	0.438015
		[86]	1.8004883	0.438714
10.0	0.70	This work	5.8826(3)	0.6105216
		[90]	5.889023	0.615473
		[86]	5.8882422	0.6161638

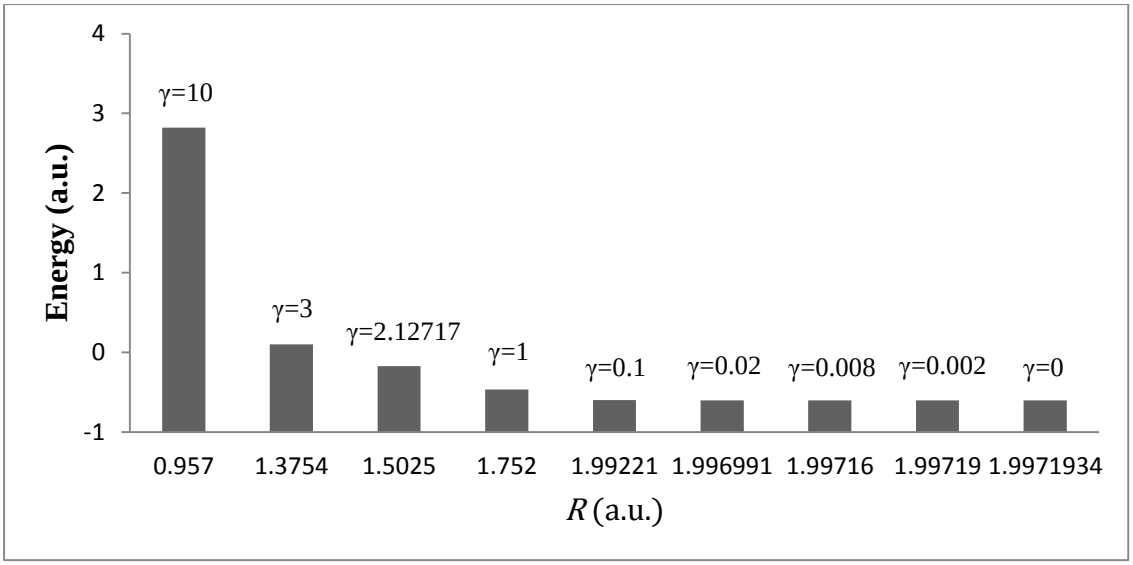

Figure-5.3 Ground-state energy of the hydrogen molecular ion H_2^+ in the presence of a magnetic field from $\gamma = 0.0$ to $\gamma = 10.0$ versus the internuclear distance R

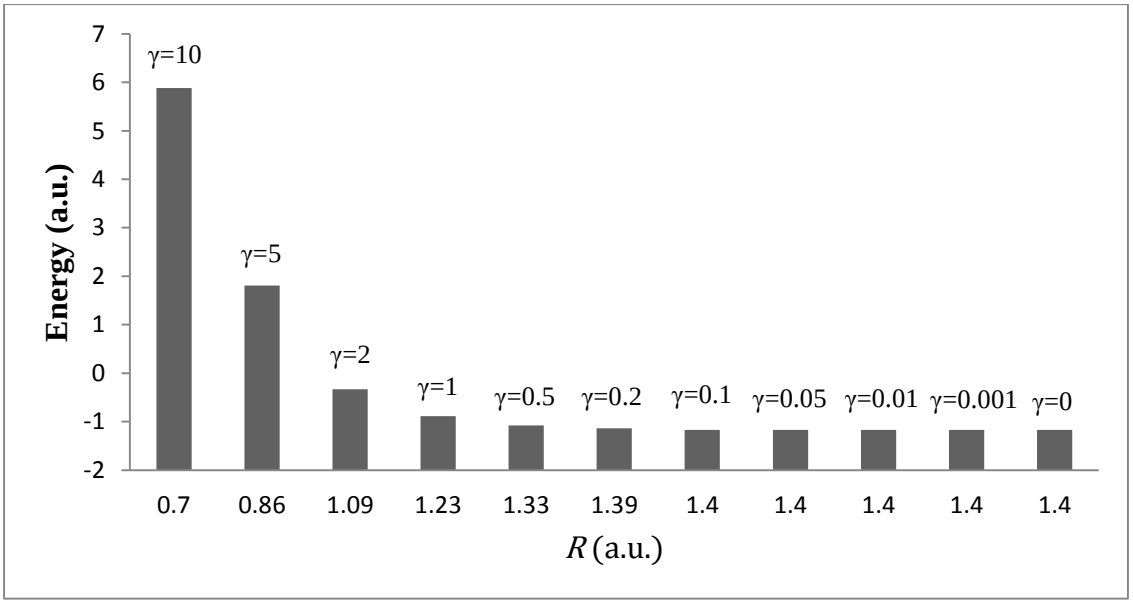

Figure-5.4 Ground-state energy of the hydrogen molecule H_2 in the presence of a magnetic field from $\gamma = 0.0$ to $\gamma = 10.0$ versus the internuclear distance R.

5.4 Conclusion

In the present chapter, we have studied the hydrogen molecular ion H_2^+ and the hydrogen molecule H_2 in the presence of a magnetic field by using the well-known variational Monte Carlo method. In the present study, the molecular axis is usually aligned along the field axis. Accordingly, we have calculated the total energies, and the dissociation energies with respect to the magnetic field for both of the hydrogen molecular ion H_2^+ and the hydrogen molecule H_2 and the binding energies for the hydrogen molecular ion H_2^+ only by using two accurate trial wave functions of the $(1s\sigma_g)$ state over various field-strength regimes. While increasing the field strength, the equilibrium distance R_{eq} decreases and the total energy, the dissociation energy, and binding energy E_b increase monotonously. In both cases our results exhibit good accuracy under various field strengths comparing with previous values obtained by using different methods and different forms of trial wave functions. This is due to the fact that we have used two trial wave functions each of them takes into consideration the electron-electron correlation. Finally, we conclude that the applications of VMC method can be extended successfully to cover the case of molecules under the effect of the magnetic field.

REFERENCES

[1] P. J. Reynolds, D. M. Ceperley, B. J. Alder, W. A. Lester, *J. Chem. Phys.* **77,** 5593, (1982).

[2] T. Kato, *Comm. Pure Appl. Math.* **10**, 151, (1957).

[3] W. M. C. Foulkes, L. Mitas, R. J. Needs, and G. Rajagopal , *Rev. Mod. Phys.* **73**, 33, (2001).

[4] R. J. Needs, M. D. Towler, N. D. Drummond, and P. Lpez Ros, *Journal of Physics: Condensed Matter*, **22**, 023201, (2010).

[5] J. Rychlewski, *int. J. Quantum Chem.* **49**, 477, (1994).

[6] R. Jastrow, *Phys. Rev.* **98**, 1479, (1955).

[7] S. Pottorf, A. Puzer, M. Y. Chou and J. E. Husbun, *Eur. J. Phys.* **20,** 205, (1999).

[8] W. L. McMillan. *Phys. Rev.* **138**, (1965).

[9] C. L. Hartmann-Siantar, R. S. Walling, T. P. Daly, B. Faddegon and N. Albright, *Med. Phys.* **28**, 1322, (2001).

[10] E. Schrödinger, *Ann. Physik.* **79**, 361, (1926).

[11] E. Schrödinger, *Ann. Physik.* **384**, 489, (1926).

[12] W. Heisenberg, *Z. Phys*. **33**, 879, (1925).

[13] P. Dirac, *Proc. Roy. Soc*. A **117**, 610, (1928).

[14] K. Manisa, *Math. Comp. Appl*. **9**, 485, (2004).

[15] A. Ma, N. D. Drummond, M. D. Towler, and R. J. Needs. *Phys. Rev. E* **71**, 066704, (2005).

[16] S. Chiesa, D. M. Ceperley, and S. Zhang. *Phys. Rev. Lett*. **94**, 036404, (2005).

[17] N. D. Drummond, P. Lopez Rios, A. Ma, J. R. Trial, G. Spink, M. D. Towler, and R. J. Needs, *J. Chem. Phys*. **124**, 224104, (2006).

[18] S. L. Davis, *J. Chem. Educ*. **84**, 711, (2007).

[19] M. D. Brown, J. R. Trial, P. Lopez, and R. J. Needs. *J. Chem. Phys.* **126**, 224110, (2007).

[20] L. Stella, C. Attaccalite, S. Sorella, A. Rubio, *Phys. Rev. B* **84**, 245117, (2011).

[21] M. Barborini, S. Sorella, and L. Guidonia, *J. Chem. Theory Comput.* **8**, 1260, (2012).

[22] A. Ambrosetti, P.L. Silvestrelli, F. Toigo, L. Mitas, F. Pederiva, *Phys. Rev. B* **85**, 0451150, (2012).

[23] T. Mizusaki and N. Shimizu, *Phys. Rev. C* **85**, 021301, (2012).

[24] N. Elkahwagy, A. Ismail, S. M. A. Maize, and K. R. Mahmoud, *JCMP*, **1**, 13, (2013).

[25] N. Elkahwagy, A. Ismail, S. M. A. Maize, and K. R. Mahmoud, *World Journal of Condensed Matter Physics*, **3**, 203, (2013).

[26] N. Elkahwagy, A. Ismail, S. M. A. Maize, and K. R. Mahmoud, *International Journal of Mathematics and Physical Sciences Research* (*IJMPSR*), **1**, 25, (2014).

[27] S. B. Doma and F. N. El-Gammal, *J. Sys. Cyber. Inf.* **7**, 78, (2009).

[28] S. B. Doma and F. N. El-Gammal, *Acta. Phys. Pol*. A **122**, 42, (2012).

[29] S. B. Doma and F. N. El-Gammal, *J. Theor. Phys*. **6**, 28, (2012).

[30] F. N. El-Gammal, *Alex. J. Math*. **2**, 1, (2011).

[31] S. B. Doma, M. O. Shaker, A. M. Farag, and F. N. El-Gammal, *Acta. Phys. Pol*. A **126**, 700, (2014).

[32] R.W. Hamming, Numerical Methods for Scientists and Engineers, 2nd ed., McGraw-Hill, New York, (1973).

[33] A. Papoulis, Probability, Random Variables, and Stochastic Processes, McGraw-Hill, New York, (1965).

[34] N. Metropolis, A. W. Rosenbluth, N. M. Rosenbluth, A. H. Teller and E. Teller, *J. Chem. Phys.* **21**, 1087, (1953).

[35] G. Bhanott, *Rep. Prog. Phys*. **51**, 429, (1988).

[36] P. Diaconis and J. W. Neuberger, *Experiment. Math*. **13**, 207, (2004).

[37] S. A. Alexandr and R. L. Coldwell, *Chemical Physics Letters*, **413**, 253, (2005).

[38] S. A. Alexandr and R. L. Coldwell, *Journal of Chemical Physics*, **121**, 11557, (2004).

[39] S. A. Alexandr and R. L. Coldwell, *International Journal of Quantum Chemistry*, **100**, 851, (2004).

[40] S. A. Alexandr and R. L. Coldwell, *International Journal of Quantum Chemistry*, **106**, 1820, (2006).

[41] S. A. Alexandr and R. L. Coldwell, *The Journal of Chemical Physics*, **129**, 114306, (2008).

[42] S. A. Alexandr and R. L. Coldwell, *International Journal of Quantum Chemistry*, **109**, 385, (2009).

[43] A. Ishikawa, H. Nakashima, and H. Nakatsuji, *J. Chem. Phys*. **128**, 124103, (2008).

[44] Y. Kurokawa, H. Nakashima, and H. Nakatsuji, *Phys. Rev. A* **72**, 062502, (2005).

[45] A. B. Suleiman and I. O. B. Ewa, *Journal of Pure and Applied Sciences*, **3**, 112, (2010).

[46] R. Colin-Rodriguez and S. A. Crus, *J. Phys. B: At. Mol. Opt. Phys.* **43**, 235102, (2010).

[47] R. Colin-Rodriguez, C. Diaz-Garcia and S. A. Crus, *J. Phys. B: At. Mol. Opt. Phys*. **44**, 241001, (2011).

[48] M. B. Ruiz and R. Schumann, *Chemical Physics Letters*, **406**, 1, (2005).

[49] H. M. James and A. S. Coolidge, *J. Chem. Phys*. **1**, 825, (1933); **3**, 129, (1935).

[50] M. M. Madsen and J. M. Peek, *At. Data*. **2**, 171, (1971).

[51] Y. X. Zhang, S. Kang, and T. Y. Shi, *Chin. Phys. Lett*. **25**, No.11, 3946, (2008).

[52] J. M. Peek, *J. Chem. Phys*. **43**, 3004, (1965).

[53] F. Weinhold and A. B. Chinen, *J. Chem. Phys*. **56**, 3798, (1972).

[54] W. Schulze and D. Kolb, *Chem. Phys. Lett.* **122**, 271, (1985).

[55] L. Laaksonen, P. Pyykko, and D. Sundholm, *Int. J. Quantum Chem*. **23**, 309, (1983).

[56] W. Kolos and C. C. J. Roothaan, *Rev. Mod. Phys*. **32,** 219, (1960).

[57] W. Kolos and L. Wolniewicz, *J. Mol. Spectrosc*. **54,** 303, (1975).

[58] J. Komasa and A. J. Thakkar, Mol. Phys, **78**, 1039, (1993).

[59] W. Kolos and L. Wolniewicz, J. Chem. Phys, **43**, 2429, (1965).

[60] S. A. Alexandr and R. L. Coldwell, *International Journal of Quantum Chemistry*, **107**, 345, (2007).

[61] A. Kaczmarek and W. Bartkowiak, *Phys. Chem. Chem. Phys*. **11**, 2885, (2009).

[62] O. P. Charkin, N. M. Klimenko and D. O. Charkin, *Adv. Quantum Chem*. **58**, 69, (2009).

[63] V. V. Struzhkin, B. Militzer, W. L. Mao, H. K. Mao and R. J. Hemley, *Chem. Rev*. **107**, 4133, (2007).

[64] Molinar-Tabares, E. Martin, Campoy-Guerena and German, *Journal of computational and Theoretical Nanoscience*, **9**, 894, (2012).

[65] S. A. Cruz and R. Colin-Rodriguez, *Int. J. Quantum Chem*. **109**, 3041, (2009).

[66] A. Sarsa, C. Le Sech, *J. Phys.* B*: At. Mol. Opt. Phys*. **45**, 205101, (2012).

[67] C. Laughlin and S. I. Chu, *J. Phys. A: Math. Theor*. **42**, 265004, (2009).

[68] S. A. Cruz, *Adv. Quantum Chem.* **57,** 255, (2009).

[69] S. Mateos-Cortes, E. Ley-Koo and S. A. Cruz, *Int. J.Quantum Chem.* **86**, 376, (2002).

[70] E. Ley-Koo and S. A. Cruz, *J. Chem. Phys*. **74**, 4603, (1981).

[71] J. Gorecki and W. Byers Brown, *J. Phys*. **89**, 2138, (1988).

[72] R. LeSar and D. R. Herschbach, *J. Phys. Chem*. **85**, 2798, (1981).

[73] R. LeSar and D. R. Herschbach, *J. Phys. Chem*. **87**, 5202, (1983).

[74] T. Pang, *Phys. Rev. A* **49**, 1709, (1994).

[75] G. Das and A. C. Wahl, *J. Chem. Phys.* **44,** 87, (1966).

[76] D. Lai, *Rev. Mod. Phys*. **73**, 629, (2001).

[77] J. Z. Yong, and L. Y. Cheng, *Chin. Phys.Soc*. **11**, 1009, (2002).

[78] X. Guan, B. Li, and K. T. Taylor, *J. Phys. B: At. Mol. Opt. Phys*. **36**, 3569, (2003).

[79] M. Vincke, and D. Baye, *J. Phys. B: At. Mol. Opt. Phys*. **39**, 2605, (2006).

[80] A. V. Turbiner, and J. C. L´opez-Vieyra, *Phys. Rep*. **424**, 309, (2006).

[81] Y. X. Zhang, S. Kang, and T. Y. Shi, *Chin. Phys. Lett*. **25**, 3946 (2008).

[82] Y.X. Zhang, Q. Liu, and T.Y. Shi, *Chin. Phys. Lett.* **30**, 043101, (2013) .

[83] Y. Zhang, Q. Liu, and T. Shi, *J. Phys. B: At. Mol. Opt. Phys*. **45,** 085101, (2012).

[84] D. Baye, A. Joos de ter Beerst, and J. M. Sparenberg, *J. Phys. B: At. Mol. Phys.* **42**, 225102, (2009).

[85] M. Sadhukhan and B. M. Deb, *J. Mol. Struct.: THEOCHEM*, **943**, 65, (2010).

[86] X. Song, H. Qiao, and X. Wang, *Phys. Rev. A* **86**, 022502, (2012).

[87] G. Ortiz, M. D. Jones, and D. M. Ceperley, *Phys. Rev. A* **52**, R3405, (1995).

[88] D. M. Larsen, *Phys. Rev.* A **25,** 1295, (1982).

[89] J. C. Lopez, P. Hess, and A. Turbiner, *Phys. Rev.* A **56,** 4496, (1997).

[90] T. Detmer, P. Schmelcher, F. K. Ddiakonos, and L. S. Cederbaum, *Phys. Rev. A* **56**, 1825, (1997).

[91] A. V. Turbiner, Pis'ma Zh. *Eksp. Teor. Fiz,* **38**, 510, (1983).

[92] U. Wille, *Phys. Rev.* A **38,** 3210, (1988).

[93] Y. P. Kravchenko, and M. A. Liberman, *Phys. Rev.* A **55,** 2701, (1997).

[94] M. S. Kaschiev, S. I. Vinitsky, and F. R. Vukajlovic, *Phys. Rev.* A **22,** 557, (1980).

[95] J. M. Peek and J. Katriel, *Phys. Rev. A* **21,** 413, (1980).

[96] M. Vincke, and D. Baye, *J. Phys. B: At. Mol. Phys.* **18,** 167, (1985).

ملخص الرسالة باللغة العربية

الهدف الأساسى من هذه الرسالة هو تطبيق طريقة مونت كارلو التقريبية للتغاير لتقديم دراسة مفصلة عن الجزيئات ثنائية الذرات و ذلك عن طريق حل معادلة شرودنجر. وكمثال على الجزيئات ثنائية الذرات قدمنا أيون جزئ الهيدروجين و جزئ الهيدروجين. حيث تم حساب طاقة المستوى الأرضى و كذلك العديد من الخواص الهامة لكل من جزئ الهيدروجين و أيون جزئ الهيدروجين. كما أمتدت الدراسة لتشمل أيون HeH^{++}. هذا ولقد تم أيضا دراسة أيون جزئ الهيدروجين و جزئ الهيدروجين تحت تأثير الإنضغاط. و أخيرا، درسنا الطاقة الكلية و طاقة الارتباط و طاقة التفكك فى حالة وجود مجال مغناطيسى خارجى.

وتحتوي هذه الرسالة على **خمسة فصول** نظمت كالتالي : المقدمة و أربع فصول و قائمة بالمراجع.

فصول الرسالة كالأتى

الفصل الأول:

في الفصل الأول من الرسالة تم تقديم مقدمة شاملة احتوت علي الخطوط العريضة للنقاط التالية: تعريف مفهوم طرق مونت كارلو بوجه عام و كذلك تقديم نبذة عن منشأ هذه الطرق و أهم تطبيقاتها فى ميكانيكا الكم و العديد من المجالات المختلفة. وقدمنا أيضا نبذة تاريخية عن منشأ معادلة شرودنجر.

الفصل الثانى:

في هذا الفصل تم إستعراض طريقة مونت كارلو للتغاير و التى هى محل الدراسة فى هذه الرسالة و من أهم طرق مونت كارلو التى تستخدم فى حل التكاملات متعددة الأبعاد. هذه الطريقة تعتمد بشكل أساسى على الجمع بين مبدأ التغاير و حساب التكاملات عن طريق أختيارأعداد عشوائية وصولا إلى حل تقريبى لحل المسائل المعقدة و قد أستعرضنا الآلية التفصيلية لخوارزمية متروبوليس (Metropolis algorithm) و الطريقة التى يتم بها ايجاد متسلسلات الأعداد العشوائية و كذلك الآلية التى يتم بناءا عليها قبول أو رفض القيم التى سوف تستخدم فى

التكامل. كذلك أستعرضنا بشئ من التفصيل الشروط الحدية التى يجب أن تحققها الدوال الموجية الحاكمة لحركة الإلكترون و تستخدم فى حل معادلة شرودنجر.

الفصل الثالث:

في هذا الفصل تم تطبيق طريقة مونت كارلو للتغاير لدراسة أيون جزئ الهيدروجين و جزئ الهيدروجين و فى هذا النسق بدأنا بحساب طاقة المستوى الأرضى و ذلك فى اطار (بورن ـ اوبنهايمر) الذى يتجاهل التأثير الناتج عن حركة النواة نظرا لكتلتها الكبيرة مقارنة بكتلة الالكترون و بالتالى يتم اهمال هذا الحد فى دالة الهاميلتونيان عند حل معادلة شرودنجر و كذلك تم حساب بعض الخصائص الجزيئية لجزئ الهيدروجين. اعتمدت الحسابات على استخدام أشكال مختلفة من الدوال الموجية و التى قدمت فى دراسات سابقة حديثة. تم عرض النتائج التى تم الحصول عليها فى جداول مقترنة بالقيم المعملية المناظرة وكذلك القيم التى تم الحصول عليها فى دراسات سابقة. وبالتالى يمكن أن نستخلص من هذه الدراسة أنه يمكن وصف الخصائص الجزيئية المختلفة بشكل دقيق و ذلك باستخدام طريقة مونت كارلو للتغاير.

الفصل الرابع:

في هذا الفصل تم تطبيق طريقة مونت كارلو للتغاير لدراسة تأثير الانضغاط على أيون جزئ الهيدروجين و جزئ الهيدروجين المحصور بجدران كروية الشكل. تم دراسة الطاقة فى حالة ثبوت الأنوية عند البؤر وحالة عدم ثبوتها. كذلك تم دراسة ايضا أيون HeH^{++} فى حالة الانضغاط. ولقد أعتمدت الحسابات على إستخدام الدوال الموجية التى تم استخدمها فى الفصل الثالث و لكن بعد إضافة الحد الذى يضمن تحقق الشروط الحدية. وتم عرض النتائج فى جداول مقترنة بالنتائج السابقة بهدف المقارنة و لقد أوضحت المقارنة أفضلية النتائج التى تم الحصول عليها بإستخدام طريقة مونت كارلو للتغاير مع النتائج السابقة.

الفصل الخامس:

في هذا الفصل تم دراسة الطاقة الكلية و طاقة الارتباط و طاقة التفكك فى المستوى الأرضى لأيون جزئ الهيدروجين و جزئ الهيدروجين تحت تأثير المجال المغناطيسى فى الفترة من القيمة (الصفرية إلى القيمة $10\ a.u.$). وتم عرض النتائج فى جداول مقترنة بالنتائج السابقة و بمقارنة النتائج يمكننا القول بأن طريقة مونت كارلو للتغاير يمكن أن توظف بنجاح لدراسة

الجزيئات تحت تأثير المجال المغناطيسى و الحصول على نتائج تحمل درجة عالية من الدقة. هذا ولقد أُختمت الرسالة بعرض المراجع المُستخدمة وكما أحتوت على ملخصا باللغة العربية.

كـلـيـة العلـــوم
قسم الرياضيــات

تطبيقات طريقة مونت كارلو للتغاير علي الجزيئات ثنائية الذرات

رسالة مقدمة إلى قسم الرياضيات– كلية العلوم– جامعة المنوفية– لاستكمال متطلبات الحصول على درجة الماجستير في العلوم شعبة (**الرياضيات التطبيقية**)

مقدمة من

أسماء عبد المغنى عبد العزيز عامر

المعيد بقسم الرياضيات– كلية العلوم– جامعة المنوفية

تحـت إشـراف

أ.د. صلاح الدين بدوي أحمد دومة

أستاذ الرياضيات التطبيقية - قسم الرياضيات
كلية العلوم - جامعة الإسكندرية
[ ]

د. محمد محمد أبوشادي

أستاذ الرياضيات التطبيقية المساعد – قسم الرياضيات
كلية العلوم – جامعة المنوفية
[ ]

د. فاطمة الزهراء نجيب الجمال

مدرس الرياضيات التطبيقية– قسم الرياضيات
كلية العلوم – جامعة المنوفية
[ ]

لجنة الحكم و المناقشة

أ.د./ محمد عمر شاكر

أستاذ الرياضيات التطبيقية– قسم الرياضيات
كلية العلوم –جامعة طنطا
[ ]

أ.د./ نبيل توفيق الضبع

أستاذ الرياضيات التطبيقية– قسم الرياضيات
كلية التربية – جامعة عين شمس
[ ]

أ.د./ صلاح الدين بدوي دومه

أستاذ الرياضيات التطبيقية– قسم الرياضيات
كلية العلوم –جامعة الأسكندرية
[ ]

د./ محمد محمد أبوشادي

أستاذ الرياضيات التطبيقية المساعد – قسم الرياضيات
كلية العلوم – جامعة المنوفية
[ ]

جمهورية مصر العربية

٢٠١٥